

A Closed-Form Control for Safety Under Input Constraints Using a Composition of Control Barrier Functions

PEDRAM RABIEE¹, JESSE B. HOAGG¹ (Senior Member, IEEE)

¹Department of Mechanical and Aerospace Engineering, University of Kentucky, Lexington, KY 40506 USA

CORRESPONDING AUTHOR: J. B. Hoagg (e-mail: jesse.hoagg@uky.edu)

This work is supported in part by the National Science Foundation (1849213,1932105) and Air Force Office of Scientific Research (FA9550-20-1-0028).

ABSTRACT We present a closed-form optimal control that satisfies both safety constraints (i.e., state constraints) and input constraints (e.g., actuator limits) using a composition of multiple control barrier functions (CBFs). This main contribution is obtained through the combination of several ideas. First, we present a method for constructing a single relaxed control barrier function (R-CBF) from multiple CBFs, which can have different relative degrees. The construction relies on a log-sum-exponential soft-minimum function and yields an R-CBF whose zero-superlevel set is a subset of the intersection of the zero-superlevel sets of all CBFs used in the composition. Next, we use the soft-minimum R-CBF to construct a closed-form control that is optimal with respect to a quadratic cost subject to the safety constraints. Finally, we use the soft-minimum R-CBF to develop a closed-form optimal control that not only guarantees safety but also respects input constraints. The key elements in developing this novel control include: the introduction of the control dynamics, which allow the input constraints to be transformed into controller-state constraints; the use of the soft-minimum R-CBF to compose multiple safety and input CBFs, which have different relative degrees; and the development of a desired surrogate control (i.e., a desired input to the control dynamics). We demonstrate these new control approaches in simulation on a nonholonomic ground robot.

INDEX TERMS Autonomous systems, constrained control, nonlinear systems and control, optimal control.

I. Introduction

Control barrier functions (CBFs) are used to determine controls that make a designated safe set forward invariant [1], [2]. Thus, CBFs can be used to generate controls that guarantee safety constraints (i.e., state constraints). CBFs are often integrated into real-time optimization-based control methods (e.g., quadratic programs) as safety filters [3]–[6]. They are also used in conjunction with stability constraints and/or performance objectives [7], [8]. Related barrier functions are used for Lyapunov-like control design and analysis (e.g., [9]–[12]). CBF methods have been demonstrated in a variety of applications, including mobile robots [13]–[16], unmanned aerial vehicles [17], [18], and autonomous vehicles [1], [19], [20].

One important challenge in CBF methods is to verify a candidate CBF, that is, confirm that the candidate CBF satisfies the conditions to be a CBF [21]. For systems without input constraints (e.g., actuator limits), a candidate CBF can

often be verified provided that it satisfies certain structural assumptions (e.g., constant relative degree) [1]. In contrast, verifying a candidate CBF under input constraints can be challenging, and this challenge is exacerbated if the safe set is described using multiple candidate CBFs. It may be possible to use offline sum-of-squares optimization methods to verify a candidate CBF [22]–[25]. Alternatively, it may be possible to synthesize a CBF offline by gridding the state space [26].

An online approach to obtain forward invariance (e.g., state constraint satisfaction) subject to input constraints is to use a prediction of the system trajectory into the future under a backup control. For example, [27], [28] determine a control forward invariant subset of the safe set by using a finite-horizon prediction of the system under a backup control. However, [27], [28] require replacing an original barrier function that describes the safe set with multiple barrier functions—one for different time instants of the

prediction horizon. Thus, the number of barrier functions increases as the prediction horizon increases, which can lead to conservative constraints and result in a set of constraints that are not simultaneously feasible. These drawbacks are addressed in [29], [30] by using a log-sum-exponential soft-minimum function to construct a single composite barrier function from the multiple barrier functions that arise from using a prediction horizon. In addition, [30] uses a log-sum-exponential soft-maximum function to allow for multiple backup controls. The use of multiple backups can enlarge the verified forward-invariant subset of the safe set. However, [27]–[30] all rely on a prediction of the system trajectories into the future. Another approach to address safety subject to input constraints is presented in [31], which uses a composition of multiple CBFs, where the composition has adaptable weights. However, the feasibility of the update law for the weights is related to the feasibility of the original optimization problem subject to input constraints. Smooth barrier function compositions (e.g., log-sum-exponential approximation of minimum and maximum) also appear in [16], [32], and nonsmooth compositions are in [33], [34].

This article presents a new approach to address forward invariance subject to input constraints. Specifically, we use the soft-minimum function to combine multiple safety constraints (i.e., state constraints) and multiple input constraints (e.g., actuator limits) into a single constraint. This composition can yield a relaxed control barrier function (R-CBF) that satisfies the CBF criteria on the boundary of its zero-superlevel set but not necessarily on the interior. This composite soft-minimum R-CBF is then used in a constrained quadratic optimization to generate a control that is optimal and satisfies both safety and input constraints. We present a closed-form control that satisfies the constrained quadratic optimization, thus eliminating the need to solve a quadratic program in real time. Closed-form solutions to other CBF-based optimizations appear in [1], [35], [36]. We also note that model predictive control methods can be used to obtain closed-form controls for systems with linear dynamics and polytopic constraints on the state and input [37]–[39]. However, extending these methods to systems with nonlinear dynamics or general nonlinear constraints typically requires solving a nonlinear optimization problem in real time. To our knowledge, this article is the first to present a closed-form CBF-based control that satisfies multiple safety constraints as well as multiple input constraints.

This new closed-form optimal control that satisfies both safety constraints and input constraints is obtained through the combination of several ideas. First, Section IV presents a method for using the soft-minimum function to construct a single R-CBF from multiple CBFs, where each CBF in the composition can have different relative degree. The zero-superlevel set of this R-CBF is a subset of the intersection of the zero-superlevel sets of all the CBFs used in the construction. Next, Section V uses the soft-minimum R-CBF and the introduction of a slack variable to construct a closed-

form optimal control that guarantees safety. The control is optimal with respect to a quadratic performance function subject to safety constraints (i.e., state constraints). The method is demonstrated on a simulation of a nonholonomic ground robot subject to position and speed constraints, which do not have the same relative degree.

Section VI presents the main contribution of this article, namely, a closed-form optimal control that not only guarantees safety (i.e., state constraints) but also respects input constraints (e.g., actuator limits). To do this, we introduce control dynamics where the control signal is an algebraic function of the controller state, and the input to the control dynamics (i.e., the surrogate control) is the closed-form solution to a constrained optimization. The use of control dynamics allows us to express the input constraints as CBFs in the state of the controller. Notably, these input-constraint CBFs do not have the same relative degree as the safety-constraint CBFs. However, this difficulty is addressed using the composite soft-minimum R-CBF construction. Lastly, we introduce a desired surrogate control (i.e., the desired input to the control dynamics) in order to convert the original optimal control problem into a surrogate optimization, where the optimization variable is the surrogate control. Other methods using control dynamics and CBFs include [40], [41]; however, neither of these address the general problem of generating an optimal control with multiple input constraints and multiple state constraints, which have potentially different relative degree. For example, [40] is limited to one state constraint and constant upper-and-lower-bound input constraints; and it does not address the optimality of the original control input. Most importantly, [40], [41] use multiple constraints that are not guaranteed to be simultaneously feasible. In contrast, this article presents a closed-form optimal control that addresses multiple state and input constraints with feasibility analysis. We demonstrate this new control method in simulations of a nonholonomic ground robot subject to position constraints, speed constraints, and input constraints—none of which have the same relative degree. Some preliminary results related to this article appear in the preliminary conference article [42]; however, [42] does not provide a comprehensive analysis (e.g., no proofs are provided). In addition, this article goes significantly beyond [42] by presenting the closed-form optimal-and-safe controls; analyzing these closed-form methods; relaxing assumptions; and providing more, discussion, examples, and simulations.

II. Notation

The interior, boundary, and closure of $\mathcal{A} \subseteq \mathbb{R}^n$ are denoted by $\text{int } \mathcal{A}$, $\text{bd } \mathcal{A}$, $\text{cl } \mathcal{A}$, respectively. Let $\text{conv } \mathcal{A}$ denote the convex hull of $\mathcal{A} \subset \mathbb{R}^n$. Let \mathbb{P}^n denote the set of symmetric positive-definite matrices in $\mathbb{R}^{n \times n}$.

Let $\eta : \mathbb{R}^n \rightarrow \mathbb{R}^\ell$ be continuously differentiable. Then, $\eta' : \mathbb{R}^n \rightarrow \mathbb{R}^{\ell \times n}$ is defined as $\eta'(x) \triangleq \frac{\partial \eta(x)}{\partial x}$. The Lie derivatives of η along the vector fields of $\psi : \mathbb{R}^n \rightarrow \mathbb{R}^{n \times m}$

is defined as

$$L_\psi \eta(x) \triangleq \eta'(x)\psi(x).$$

If $m = 1$, then for all positive integers d , define

$$L_\psi^d \eta(x) \triangleq L_\psi L_\psi^{d-1} \eta(x).$$

Throughout this paper, we assume that all functions are sufficiently smooth such that all derivatives that we write exist and are continuous.

A continuous function $a: \mathbb{R} \rightarrow \mathbb{R}$ is an *extended class- \mathcal{K} function* if it is strictly increasing and $a(0) = 0$.

Let $\rho > 0$, and consider $\text{softmin}_\rho: \mathbb{R}^N \rightarrow \mathbb{R}$ defined by

$$\text{softmin}_\rho(z_1, \dots, z_N) \triangleq -\frac{1}{\rho} \log \sum_{i=1}^N e^{-\rho z_i}, \quad (1)$$

which is the log-sum-exponential *soft minimum*. The next result relates the soft minimum to the minimum. The proof is in Appendix A.

Proposition 1. Let $z_1, \dots, z_N \in \mathbb{R}$. Then,

$$\begin{aligned} \min \{z_1, \dots, z_N\} - \frac{\log N}{\rho} &\leq \text{softmin}_\rho(z_1, \dots, z_N) \\ &\leq \min \{z_1, \dots, z_N\}. \end{aligned}$$

Proposition 1 demonstrates that softmin_ρ lower bounds the minimum, and converges to the minimum as $\rho \rightarrow \infty$. Thus, softmin_ρ is a smooth approximation of the minimum. Note that if $N > 1$, then the soft minimum is strictly less than the minimum.

III. Problem Formulation

Consider

$$\dot{x}(t) = f(x(t)) + g(x(t))u(x(t)), \quad (2)$$

where $x(t) \in \mathbb{R}^n$ is the state, $x(0) = x_0 \in \mathbb{R}^n$ is the initial condition, $f: \mathbb{R}^n \rightarrow \mathbb{R}^n$ and $g: \mathbb{R}^n \rightarrow \mathbb{R}^{n \times m}$ are locally Lipschitz continuous on \mathbb{R}^n , and $u: \mathbb{R}^n \rightarrow \mathbb{R}^m$ is the control, which is locally Lipschitz continuous on \mathbb{R}^n .

Since f , g , and u are locally Lipschitz, it follows that for all $x_0 \in \mathbb{R}^n$, there exists a maximum value $t_{\max}(x_0) \in [0, \infty)$ such that $x(t)$ is the unique solution to (2) on $I(x_0) \triangleq [0, t_{\max}(x_0))$.

A. Preliminary Definitions and Results

The following definitions are needed. The first definition is similar to [43, Definition 4.4]. The second definition is a standard definition of a CBF (for example, see [1, Definition 5]), and the third definition is a relaxation of the standard CBF definition.

Definition 1. A set $\mathcal{D} \subset \mathbb{R}^n$ is *control forward invariant* with respect to (2) if there exists a locally Lipschitz $u_i: \mathcal{D} \rightarrow \mathbb{R}^m$ such that for all $x_0 \in \mathcal{D}$, the solution x to (2) with $u = u_i$ is such that for all $t \in I(x_0)$, $x(t) \in \mathcal{D}$.

Definition 2. Let $\eta: \mathbb{R}^n \rightarrow \mathbb{R}$ be continuously differentiable, and define $\mathcal{D} \triangleq \{x \in \mathbb{R}^n: \eta(x) \geq 0\}$. Then, η is a *control barrier function* (CBF) for (2) on \mathcal{D} if there exists an

extended class- \mathcal{K} function $a: \mathbb{R} \rightarrow \mathbb{R}$ such that for all $x \in \mathcal{D}$,

$$\sup_{u \in \mathbb{R}^m} L_f \eta(x) + L_g \eta(x)u + a(\eta(x)) \geq 0. \quad (3)$$

Definition 3. Let $\eta: \mathbb{R}^n \rightarrow \mathbb{R}$ be continuously differentiable, and define $\mathcal{D} \triangleq \{x \in \mathbb{R}^n: \eta(x) \geq 0\}$. Then, η is a *relaxed control barrier function* (R-CBF) for (2) on \mathcal{D} if for all $x \in \text{bd } \mathcal{D}$,

$$\sup_{u \in \mathbb{R}^m} L_f \eta(x) + L_g \eta(x)u \geq 0. \quad (4)$$

Definition 3 implies that an R-CBF need only satisfy (4) on the boundary of its zero-superlevel. In contrast, Definition 2 implies that a CBF must satisfy (3) on the boundary as well as the interior of its zero-superlevel set. Note that every CBF is an R-CBF. CBF definitions often take the supremum (3) over a subset of \mathbb{R}^m based on control limits. Nevertheless, Definitions 2 and 3 are adequate for this article because we do not require CBFs or R-CBFs where the input variable is constrained to a subset of \mathbb{R}^m even though Section VI addresses control constraints.

The following result provides sufficient conditions for η to be an R-CBF. The result also provides sufficient conditions for the zero-superlevel set of η to be control forward invariant.

Lemma 1. Let $\eta: \mathbb{R}^n \rightarrow \mathbb{R}$ be continuously differentiable, and define $\mathcal{D} \triangleq \{x \in \mathbb{R}^n: \eta(x) \geq 0\}$. Assume that for all $x \in \text{bd } \mathcal{D}$, if $L_f \eta(x) \leq 0$, then $L_g \eta(x) \neq 0$. Then, the following statements hold:

- (a) η is an R-CBF for (2) on \mathcal{D} .
- (b) If η' is locally Lipschitz on \mathcal{D} , then \mathcal{D} is control forward invariant with respect to (2).

Proof:

To prove (a), consider $u_i: \mathcal{D} \rightarrow \mathbb{R}^m$ defined by

$$u_i(x) \triangleq \begin{cases} \frac{-L_f \eta(x) L_g \eta(x)^T}{L_g \eta(x) L_g \eta(x)^T + \eta(x)^2}, & L_f \eta(x) < 0, \\ 0, & L_f \eta(x) \geq 0. \end{cases} \quad (5)$$

and it follows that for all $x \in \text{bd } \mathcal{D}$,

$$L_f \eta(x) + L_g \eta(x)u_i(x) = \begin{cases} 0, & L_f \eta(x) < 0, \\ L_f \eta(x), & L_f \eta(x) \geq 0. \end{cases} \quad (6)$$

Thus, (6) implies that for all $x \in \text{bd } \mathcal{D}$, $L_f \eta(x) + L_g \eta(x)u_i(x) \geq 0$, and it follows from Definition 3 that η is an R-CBF.

To prove (b), since $L_g \eta(x) \neq 0$ for all $x \in \{a \in \text{bd } \mathcal{D}: L_f \eta(a) \leq 0\}$, it follows from (5) that u_i is continuous on \mathcal{D} . Since, in addition, f , g , and η' are locally Lipschitz on \mathcal{D} , it follows from (5) that u_i is locally Lipschitz on \mathcal{D} . Next, consider (2) with $u = u_i$ and $x_0 \in \mathcal{D}$. Since for all $x \in \text{bd } \mathcal{D}$, $L_f \eta(x) + L_g \eta(x)u_i(x) \geq 0$, it follows from Nagumo's Theorem [43, Theorem 4.7] that for all $t \in I(x_0)$, $x(t) \in \mathcal{D}$. Thus, Definition 1 implies that \mathcal{D} is control forward invariant. ■

B. Control Objective

Let $h_1, h_2, \dots, h_\ell: \mathbb{R}^n \rightarrow \mathbb{R}$ be continuously differentiable, and for all $j \in \{1, 2, \dots, \ell\}$, define

$$\mathcal{C}_{j,0} \triangleq \{x \in \mathbb{R}^n: h_j(x) \geq 0\}. \quad (7)$$

The *safe set* is

$$\mathcal{S}_s \triangleq \bigcap_{j=1}^{\ell} \mathcal{C}_{j,0}. \quad (8)$$

Unless otherwise stated, all statements in this paper that involve the subscript j are for all $j \in \{1, 2, \dots, \ell\}$. We make the following assumption:

- (A1) There exists a positive integer d_j such that for all $x \in \mathbb{R}^n$ and all $i \in \{0, 1, \dots, d_j - 2\}$, $L_g L_f^i h_j(x) = 0$; and for all $x \in \mathcal{S}_s$, $L_g L_f^{d_j-1} h_j(x) \neq 0$.

Assumption (A1) implies h_j has well-defined relative degree d_j with respect to (2) on \mathcal{S}_s ; however, relative degrees d_1, \dots, d_ℓ need not be equal. Assumption (A1) also implies that h_j is a relative-degree- d_j CBF. However, we do not assume knowledge of a CBF for the safe set \mathcal{S}_s . Section IV presents a method for constructing a single composite R-CBF from h_1, \dots, h_ℓ , which can have different relative degrees.

Consider the cost function $J: \mathbb{R}^n \times \mathbb{R}^m \rightarrow \mathbb{R}$ defined by

$$J(x, u) \triangleq \frac{1}{2} u^T Q(x) u + c(x)^T u, \quad (9)$$

where $Q: \mathbb{R}^n \rightarrow \mathbb{P}^m$ and $c: \mathbb{R}^n \rightarrow \mathbb{R}^m$ are locally Lipschitz continuous on \mathbb{R}^n .

The control objective is to design a full-state feedback control $u: \mathbb{R}^n \rightarrow \mathbb{R}^m$ such that for all $t \in I(x_0)$, $J(x(t), u(x(t)))$ is minimized subject to the safety constraint that $x(t) \in \mathcal{S}_s$. Section V presents a closed-form control that satisfies these objectives. Then, Section VI presents a closed-form control that satisfies these objectives and satisfies control input constraints.

A special case of this optimal control problem is the minimum-intervention problem, where we consider a desired control $u_d: \mathbb{R}^n \rightarrow \mathbb{R}^m$ that is designed to satisfy performance requirements but may not account for safety. In this case, the objective is to design a feedback control such that the minimum-intervention cost $\|u - u_d(x(t))\|_2^2$ is minimized subject to the safety constraint and potentially subject to control input constraints. The minimum-intervention cost $\|u - u_d(x)\|_2^2$ is minimized by $u_d(x)$, which is equal to the minimizer of (9) with $Q(x) = I_m$ and $c(x) = -u_d(x)$. Thus, the minimum-intervention problem is addressed by letting $Q(x) = I_m$ and $c(x) = -u_d(x)$.

Although the cost (9) is quadratic in u , nonquadratic cost functions can often be approximated locally by quadratic forms. This quadratic approximation technique is commonly used in differential dynamic programming (e.g., [44]). Thus, the method in this paper can be implemented effectively in some cases where the cost is not quadratic in u .

IV. Composite Soft-Minimum R-CBF

This section presents a method for constructing a single composite R-CBF from multiple CBFs (i.e., h_1, \dots, h_ℓ), which can have different relative degrees.

Let $b_{j,0}(x) \triangleq h_j(x)$. For $i \in \{0, 1, \dots, d_j - 2\}$, let $\alpha_{j,i}: \mathbb{R} \rightarrow \mathbb{R}$ be a locally Lipschitz extended class- \mathcal{K} function, and consider $b_{j,i+1}: \mathbb{R}^n \rightarrow \mathbb{R}$ defined by

$$b_{j,i+1}(x) \triangleq L_f b_{j,i}(x) + \alpha_{j,i}(b_{j,i}(x)). \quad (10)$$

For $i \in \{1, \dots, d_j - 1\}$, define

$$\mathcal{C}_{j,i} \triangleq \{x \in \mathbb{R}^n: b_{j,i}(x) \geq 0\}. \quad (11)$$

Next, define

$$\mathcal{C}_j \triangleq \begin{cases} \mathcal{C}_{j,0}, & d_j = 1, \\ \bigcap_{i=0}^{d_j-2} \mathcal{C}_{j,i}, & d_j > 1, \end{cases} \quad (12)$$

and

$$\mathcal{C} \triangleq \bigcap_{j=1}^{\ell} \mathcal{C}_j. \quad (13)$$

Note that $\mathcal{C} \subseteq \mathcal{S}_s$. In addition, note that if $d_1, \dots, d_\ell \in \{1, 2\}$, then $\mathcal{C} = \mathcal{S}_s$.

The next result is from [45, Proposition 1] and provides a sufficient condition such that \mathcal{C}_j is forward invariant.

Lemma 2. Consider (2), where (A1) is satisfied. Let $j \in \{1, \dots, \ell\}$. Assume $x_0 \in \mathcal{C}_j$, and assume for all $t \in I(x_0)$, $b_{j,d_j-1}(x(t)) \geq 0$. Then, for all $t \in I(x_0)$, $x(t) \in \mathcal{C}_j$.

Lemma 2 implies that if $x_0 \in \mathcal{C}$ and for all $j \in \{1, \dots, \ell\}$ and all $t \in I(x_0)$, $b_{j,d_j-1}(x(t)) \geq 0$, then for all $t \in I(x_0)$, $x(t) \in \mathcal{C} \subseteq \mathcal{S}_s$. This motivates us to consider a candidate R-CBF whose zero-superlevel set approximates the intersection of the zero-superlevel sets of $b_{1,d_1-1}, \dots, b_{\ell,d_\ell-1}$. Specifically, let $\rho > 0$, and consider the candidate R-CBF $h: \mathbb{R}^n \rightarrow \mathbb{R}$ defined by

$$h(x) \triangleq \text{softmin}_\rho \left(b_{1,d_1-1}(x), b_{2,d_2-1}(x), \dots, b_{\ell,d_\ell-1}(x) \right). \quad (14)$$

The zero-superlevel set of h is

$$\mathcal{H} \triangleq \{x \in \mathbb{R}^n: h(x) \geq 0\}. \quad (15)$$

The next result is the immediate consequence of Proposition 1 and demonstrates that \mathcal{H} is a subset of the intersection of the zero-superlevel sets of $b_{1,d_1-1}, \dots, b_{\ell,d_\ell-1}$.

Proposition 2. $\mathcal{H} \subseteq \bigcap_{j=1}^{\ell} \mathcal{C}_{j,d_j-1}$.

Proposition 1 also implies that \mathcal{H} approximates the intersection of the zero-superlevel sets of $b_{1,d_1-1}, \dots, b_{\ell,d_\ell-1}$ in the sense that as $\rho \rightarrow \infty$, $\mathcal{H} \rightarrow \bigcap_{j=1}^{\ell} \mathcal{C}_{j,d_j-1}$. In other words, Proposition 1 shows that for sufficiently large $\rho > 0$, h is a smooth approximation of $\min \{b_{1,d_1-1}, \dots, b_{\ell,d_\ell-1}\}$. If $\rho > 0$ is small, then h is a conservative approximation of $\min \{b_{1,d_1-1}, \dots, b_{\ell,d_\ell-1}\}$. However, if $\rho > 0$ is large, then $\|h'(x)\|_2$ is large at points where $\min \{b_{1,d_1-1}, \dots, b_{\ell,d_\ell-1}\}$ is not differentiable. Thus, selecting ρ is a trade-off between the conservativeness of h and the size of $\|h'(x)\|_2$.

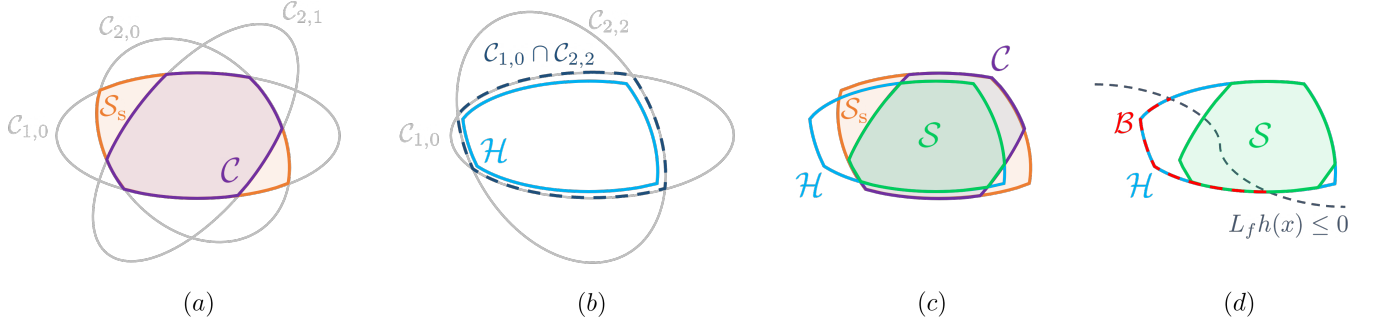


FIGURE 1. Illustration of the relationships between \mathcal{S}_s , \mathcal{C} , \mathcal{H} , and \mathcal{S} for $\ell = 2$ with $d_1 = 1$ and $d_2 = 3$. (a) shows $\mathcal{S}_s = \mathcal{C}_{1,0} \cap \mathcal{C}_{2,0}$ and $\mathcal{C} = \mathcal{C}_{1,0} \cap \mathcal{C}_{2,0} \cap \mathcal{C}_{2,1}$. (b) shows $\mathcal{C}_{1,0} \cap \mathcal{C}_{2,2}$ and $\mathcal{H} \subset \mathcal{C}_{1,0} \cap \mathcal{C}_{2,2}$. (c) shows \mathcal{S}_s , \mathcal{C} , \mathcal{H} , and $\mathcal{S} \triangleq \mathcal{C} \cap \mathcal{H}$. (d) shows \mathcal{H} , \mathcal{S} and $\mathcal{B} \triangleq \{x \in \text{bd } \mathcal{H}: L_f h(x) \leq 0\}$.

Note that \mathcal{H} is not generally a subset of \mathcal{S}_s or \mathcal{C} . In the special case where $d_1 = \dots = d_\ell = 1$, it follows that $\mathcal{H} \subseteq \mathcal{C} = \mathcal{S}_s$, and as $\rho \rightarrow \infty$, $\mathcal{H} \rightarrow \mathcal{S}_s$.

Next, we define

$$\mathcal{S} \triangleq \mathcal{H} \cap \mathcal{C}, \quad (16)$$

and since $\mathcal{C} \subseteq \mathcal{S}_s$, it follows that $\mathcal{S} \subseteq \mathcal{S}_s$.

To illustrate the relationship between \mathcal{S}_s , \mathcal{C} , \mathcal{H} , and \mathcal{S} , we consider the case where $\ell = 2$, $d_1 = 1$, and $d_2 = 3$. In this case, $b_{1,0} = h_1$, $b_{2,0} = h_2$, and $b_{2,1}$ and $b_{2,2}$ are defined by (10). First, it follows from (8) that $\mathcal{S}_s = \mathcal{C}_{1,0} \cap \mathcal{C}_{2,0}$. Next, it follows from (11)–(13) that $\mathcal{C} = \mathcal{C}_1 \cap \mathcal{C}_2 = \mathcal{C}_{1,0} \cap \mathcal{C}_{2,0} \cap \mathcal{C}_{2,1}$. Thus, $\mathcal{C} \subset \mathcal{S}_s$ as shown in Figure 1(a). For this example, (14) implies that $h(x) = \text{softmin}_\rho(b_{1,0}(x), b_{2,2}(x))$, and it follows from Proposition 2 that $\mathcal{H} \subset \mathcal{C}_{1,0} \cap \mathcal{C}_{2,2}$ as shown in Figure 1(b). Finally, as shown in Figure 1(c), \mathcal{H} is not necessarily a subset of \mathcal{S}_s , but $\mathcal{S} = \mathcal{H} \cap \mathcal{C}$ is a subset of \mathcal{S}_s .

Next, define

$$\begin{aligned} \mathcal{B} &\triangleq \{x \in \text{bd } \mathcal{H}: L_f h(x) \leq 0\} \\ &= \{x \in \mathbb{R}^n: L_f h(x) \leq 0 \text{ and } h(x) = 0\}, \end{aligned} \quad (17)$$

which is shown in Figure 1(d). Lemma 1 implies that if $L_g h$ is nonzero on \mathcal{B} , then h is an R-CBF. Lemma 1 also implies that if $L_g h$ is nonzero on \mathcal{B} and h' is locally Lipschitz, then \mathcal{H} is control forward invariant. The next result shows that in this case not only is \mathcal{H} control forward invariant but \mathcal{S} is also control forward invariant. This fact is significant because \mathcal{S} is a subset of the safe set \mathcal{S}_s , whereas \mathcal{H} is not necessarily a subset of \mathcal{S}_s .

Proposition 3. Consider (2), where (A1) is satisfied. Assume that h' is locally Lipschitz on \mathcal{H} , and for all $x \in \mathcal{B}$, $L_g h(x) \neq 0$. Then, \mathcal{S} is control forward invariant.

Proof:

Let $x_0 \in \mathcal{S}$. Since h' is locally Lipschitz on \mathcal{H} , and for all $x \in \mathcal{B}$, $L_g h(x) \neq 0$, it follows from Lemma 1 that \mathcal{H} is control forward invariant. Since, in addition, $x_0 \in \mathcal{S} \subseteq \mathcal{H}$, it follows from Definition 1 that there exists a locally Lipschitz $u_i: \mathcal{H} \rightarrow \mathbb{R}^m$ such that the solution to (2) with $u = u_i$ is such that for all $t \in I(x_0)$, $x(t) \in \mathcal{H}$, which implies $h(x(t)) \geq 0$. Thus, (15), Proposition 2, and (11) imply that

for all $t \in I(x_0)$, $b_{j,d_j-1}(x(t)) \geq 0$. Since, in addition, $x_0 \in \mathcal{S} \subseteq \mathcal{C}_j$, it follows from Lemma 2 that for all $t \in I(x_0)$, $x(t) \in \mathcal{C}_j$. Thus, for all $t \in I(x_0)$, $x(t) \in \mathcal{C}$, which implies that for all $t \in I(x_0)$, $x(t) \in \mathcal{S} = \mathcal{H} \cap \mathcal{C}$. ■

Remark 1. Proposition 3 provides a sufficient condition such that \mathcal{S} is control forward invariant. However, Figure 1(d) illustrates that it is not necessary that $L_g h(x) \neq 0$ for all $x \in \mathcal{B}$. Specifically, it suffices that for all $x \in \mathcal{B} \cap \mathcal{S}$, $L_g h(x) \neq 0$.

The conditions in Proposition 3 guarantee that $\mathcal{S} \subseteq \mathcal{S}_s$ is control forward invariant and h is an R-CBF. In this case, h is not necessarily a CBF. Under additional assumptions (e.g., \mathcal{H} is compact), h may be a CBF. However, even if h is a CBF, it can be difficult to determine an associated extended class- \mathcal{K} function $a: \mathbb{R} \rightarrow \mathbb{R}$ that satisfies Definition 2. The next section presents an optimal and safe control using the R-CBF h . This approach does not require that h is CBF, and thus, does not require knowledge of an associated function a .

V. Closed-Form Optimal and Safe Control

This section uses the composite soft-minimum R-CBF (14) to construct a closed-form optimal control that guarantees safety. Specifically, we design an optimal control subject to the constraint that $x(t) \in \mathcal{S} \subseteq \mathcal{S}_s$.

Let $\gamma > 0$, and let $\alpha: \mathbb{R} \rightarrow \mathbb{R}$ be a locally Lipschitz nondecreasing function such that $\alpha(0) = 0$. For all $x \in \mathbb{R}^n$, consider the control given by

$$(u(x), \mu(x)) \triangleq \underset{\tilde{u} \in \mathbb{R}^m, \tilde{\mu} \in \mathbb{R}}{\text{argmin}} J(x, \tilde{u}) + \frac{1}{2} \gamma \tilde{\mu}^2 \quad (18a)$$

subject to

$$L_f h(x) + L_g h(x) \tilde{u} + \alpha(h(x)) + \tilde{\mu} h(x) \geq 0. \quad (18b)$$

The quadratic program (18) includes the slack variable $\tilde{\mu}$ because h is an R-CBF but not necessarily a CBF. A typical CBF-based constraint does not include the slack-variable term $\tilde{\mu} h(x)$ in (18b). In this case, additional assumptions are needed to ensure that (18b) is feasible. For example, it is common to require that h is a CBF and that α is an extended class- \mathcal{K} function that satisfies Definition 2 with $\eta = h$ and $a = \alpha$. Since h is only an R-CBF, the slack variable $\tilde{\mu}$ ensures that for all $x \notin \mathcal{B}$, (18b) is feasible. Hence, if $L_g h$

is nonzero on \mathcal{B} , then (18b) is feasible for all $x \in \mathbb{R}^n$. The next result formalizes this fact. Specifically, it shows that if for all $x \in \mathcal{B}$, $L_g h(x) \neq 0$, then the quadratic program (18) is feasible on \mathbb{R}^n .

Proposition 4. The following statements hold:

- (a) Let $x \in \mathbb{R}^n \setminus \mathcal{H}$. Then, there exists $\tilde{u} \in \mathbb{R}^m$ and $\tilde{\mu} \in \mathbb{R}$ such that (18b) is satisfied.
- (b) Let $x \in \mathcal{H} \setminus \mathcal{B}$. Then, there exists $\tilde{u} \in \mathbb{R}^m$ and $\tilde{\mu} \geq 0$ such that (18b) is satisfied.
- (c) Let $x \in \mathcal{B}$. If $L_g h(x) \neq 0$, then there exists $\tilde{u} \in \mathbb{R}^m$ and $\tilde{\mu} \geq 0$ such that (18b) is satisfied.

Proof:

To prove (a), let $x_1 \in \mathbb{R}^n \setminus \mathcal{H}$, which implies that $h(x_1) < 0$. Thus, $\tilde{u} = 0$ and $\tilde{\mu} = -[L_f h(x_1) + \alpha(h(x_1))]/h(x_1)$ satisfy (18b).

To prove (b), let $x_2 \in (\text{bd } \mathcal{H}) \setminus \mathcal{B}$, which implies that $h(x_2) = 0$ and $L_f h(x_2) > 0$. Thus, $\tilde{u} = 0$ and $\tilde{\mu} = 0$ satisfy (18b). Next, let $x_3 \in \text{int } \mathcal{H}$, which implies that $h(x_3) > 0$. Thus, $\tilde{u} = 0$ and $\tilde{\mu} = \max\{-[L_f h(x_3) + \alpha(h(x_3))]/h(x_3), 0\} \geq 0$ satisfy (18b).

To prove (c), let $x_4 \in \mathcal{B}$, which implies that $h(x_4) = 0$. Since $L_g h(x_4) \neq 0$, it follows that $\tilde{u} = -L_f h(x_4)/L_g h(x_4)$ and $\tilde{\mu} = 0$ satisfy (18b). ■

The user-selected parameter $\gamma > 0$ influences the behavior of the control u that satisfies (18). Specifically, γ weights the slack-variable term in the cost $J(x, \tilde{u}) + \frac{1}{2}\gamma\tilde{\mu}^2$. For small γ (e.g., as $\gamma \rightarrow 0$), the control u that satisfies (18) is aggressive in the sense that it is approximately equal to $-Q^{-1}c$, which is the unconstrained minimizer of J , except for x near the boundary of \mathcal{H} . For large γ (e.g., as $\gamma \rightarrow \infty$), the control u that satisfies (18) is similar to the control generated by a quadratic program that does not include the slack-variable term in (18b). In this case, the aggressiveness of the control is determined by the nondecreasing function α and the extended class- \mathcal{K} functions $\alpha_{j,0}, \dots, \alpha_{j,d_j-2}$.

In order to present a closed-form solution to the quadratic program (18), consider $\omega : \mathbb{R}^n \rightarrow \mathbb{R}$ defined by

$$\omega(x) \triangleq L_f h(x) - L_g h(x)Q(x)^{-1}c(x) + \alpha(h(x)), \quad (19)$$

and define

$$\Omega \triangleq \{x \in \mathbb{R}^n : \omega(x) < 0\}. \quad (20)$$

The following result provides a closed-form solution for the unique global minimizer $(u(x), \mu(x))$ of the constrained optimization (18). This result also shows that if h' is locally Lipschitz, then u and μ are locally Lipschitz.

Theorem 1. Assume that for all $x \in \mathcal{B}$, $L_g h(x) \neq 0$. Then, the following hold:

- (a) For all $x \in \mathbb{R}^n$,

$$u(x) = -Q(x)^{-1}(c(x) - L_g h(x)^T \lambda(x)), \quad (21)$$

$$\mu(x) = \frac{h(x)\lambda(x)}{\gamma}, \quad (22)$$

where $\lambda : \mathbb{R}^n \rightarrow \mathbb{R}$ is defined by

$$\lambda(x) \triangleq \begin{cases} \frac{-\omega(x)}{d(x)}, & x \in \Omega, \\ 0, & x \notin \Omega, \end{cases} \quad (23)$$

and $d : \Omega \rightarrow \mathbb{R}$ is defined by

$$d(x) \triangleq L_g h(x)Q(x)^{-1}L_g h(x)^T + \gamma^{-1}h(x)^2. \quad (24)$$

- (b) For all $x \in \mathbb{R}^n$, $\lambda(x) \geq 0$, and for all $x \in \mathcal{H}$, $\mu(x) \geq 0$.
- (c) u , μ , and λ are continuous on \mathbb{R}^n .
- (d) Let $\mathcal{D} \subseteq \mathbb{R}^n$, and assume that h' is locally Lipschitz on \mathcal{D} . Then, u , μ , and λ are locally Lipschitz on \mathcal{D} .

Proof:

First, we show that for all $x \in \text{cl } \Omega$, $d(x) > 0$. Let $a \in \text{cl } \Omega$, and assume for contradiction that $d(a) = 0$. Since $\gamma > 0$ and Q is positive definite, it follows from (24) that $L_g h(a) = 0$ and $h(a) = 0$. Since, in addition, for all $x \in \mathcal{B}$, $L_g h(x) \neq 0$, it follows from (17) that $L_f h(a) > 0$. Thus, (19) implies $\omega(a) = L_f h(a) > 0$, which implies $a \notin \text{cl } \Omega$, which is a contradiction. Thus, $d(a) \neq 0$, which implies that $d(a) > 0$. Thus, for all $x \in \text{cl } \Omega$, $d(x) > 0$.

To prove (a), define

$$\tilde{J}(x, \tilde{u}, \tilde{\mu}) \triangleq J(x, \tilde{u}) + \frac{1}{2}\gamma\tilde{\mu}^2,$$

$$b(x, \tilde{u}, \tilde{\mu}) \triangleq L_f h(x) + L_g h(x)\tilde{u} + \alpha(h(x)) + \tilde{\mu}h(x),$$

$$u_*(x) \triangleq -Q(x)^{-1}c(x),$$

and note that u_* is the unique global minimizer of J , which implies that $(u_*, 0)$ is the unique global minimizer of \tilde{J} .

First, let $x_1 \notin \Omega$, and it follows from (20) that $\omega(x_1) \geq 0$, which combined with (19) implies that $(\tilde{u}, \tilde{\mu}) = (u_*(x_1), 0)$ satisfies (18b). Since, in addition, $(\tilde{u}, \tilde{\mu}) = (u_*(x_1), 0)$ is the unique global minimizer of $\tilde{J}(x_1, \tilde{u}, \tilde{\mu})$, it follows that $(\tilde{u}, \tilde{\mu}) = (u_*(x_1), 0)$ is the solution to (18). Finally, (21)–(24) yields $u(x_1) = u_*(x_1)$ and $\mu(x_1) = 0$, which confirms (a) for all $x \notin \Omega$.

Next, let $x_2 \in \Omega$. Let $(u_2, \mu_2) \in \mathbb{R}^m \times \mathbb{R}$ denote the the unique global minimizer of $\tilde{J}(x_2, \tilde{u}, \tilde{\mu})$ subject to $b(x_2, \tilde{u}, \tilde{\mu}) \geq 0$. Since $x_2 \in \Omega$, it follows from (19) that $b(x_2, u_*(x_2), 0) = \omega(x_2) < 0$. Thus, $b(x_2, u_2, \mu_2) = 0$. Define the Lagrangian

$$\mathcal{L}(\tilde{u}, \tilde{\mu}, \tilde{\lambda}) \triangleq \tilde{J}(x_2, \tilde{u}, \tilde{\mu}) - \tilde{\lambda}b(x_2, \tilde{u}, \tilde{\mu}).$$

Let $\lambda_2 \in \mathbb{R}$ be such that (u_2, μ_2, λ_2) is a stationary point of \mathcal{L} . Evaluating $\frac{\partial \mathcal{L}}{\partial \tilde{u}}$, $\frac{\partial \mathcal{L}}{\partial \tilde{\mu}}$, and $\frac{\partial \mathcal{L}}{\partial \tilde{\lambda}}$ at (u_2, μ_2, λ_2) ; setting equal to zero; and solving for u_2 , μ_2 , and λ_2 yields

$$u_2 = -Q(x_2)^{-1}(c(x_2) - L_g h(x_2)^T \lambda_2),$$

$$\mu_2 = \frac{h(x_2)\lambda_2}{\gamma},$$

$$\lambda_2 = \frac{-\omega(x_2)}{d(x_2)},$$

where $d(x_2) \neq 0$ because $x_2 \in \Omega$. Finally, (21)–(24) yields $u(x_2) = u_2$, $\mu(x_2) = \mu_2$, and $\lambda(x_2) = \lambda_2$, which confirms (a) for all $x \in \Omega$.

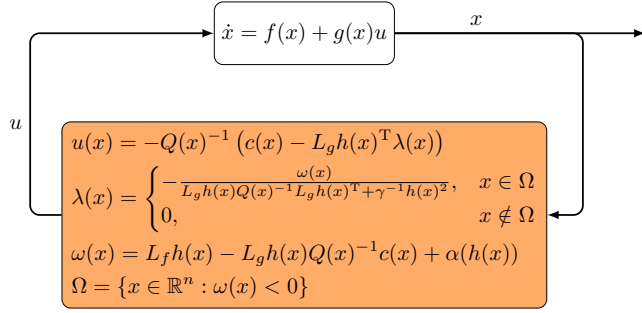


FIGURE 2. Closed-form optimal and safe control using the composite soft-minimum R-CBF (14). Control minimizes cost subject to safety constraint.

To prove (b), since d is positive on $\text{cl } \Omega$, it follows from (19), (20), and (23) that for all $x \in \mathbb{R}^n$, $\lambda(x) \geq 0$. Since, in addition, $\gamma > 0$ and h is nonnegative on \mathcal{S} , it follows from (22) that for all $x \in \mathcal{H}$, $\mu(x) \geq 0$.

To prove (c), let $a \in \text{bd } \Omega$, which implies that $\omega(a) = 0$ and $d(a) > 0$. Thus, $-\omega(a)/d(a) = 0$, and (23) implies that λ is continuous on $\text{bd } \Omega$. Since, in addition, f , g , Q^{-1} , c , h , and h' are continuous on \mathbb{R}^n , it follows from (19), (23), and (24) that λ is continuous on \mathbb{R}^n , which combined with (21) and (22) implies that u and μ are continuous on \mathbb{R}^n .

To prove (d), note that f , g , Q^{-1} , c , α and h are locally Lipschitz on \mathbb{R}^n . Since h' is locally Lipschitz on \mathcal{D} , it follows from (19) and (24) that ω and d are locally Lipschitz on \mathcal{D} . Thus, (23) implies that λ is locally Lipschitz on \mathcal{D} , which combined with (21) and (22) implies that u and μ are locally Lipschitz on \mathcal{D} . ■

Figure 2 is a block diagram of the control (10), (14), and (19)–(24), which is the closed-form solution to the quadratic program (18). The control depends on the user-selected parameter $\gamma > 0$ and the user-selected functions α and $\alpha_{j,1}, \dots, \alpha_{j,d_j-2}$, which are similar to the extended class- \mathcal{K} functions used in a typical higher-order CBF-based constraint. The parameter γ and the function α influence the aggressiveness of the control. The functions $\alpha_{j,1}, \dots, \alpha_{j,d_j-2}$ influence the aggressiveness of the control as well as the size of \mathcal{C} and thus, the size of the control forward invariant set $\mathcal{S} = \mathcal{H} \cap \mathcal{C}$.

The control (10), (14), and (19)–(24) requires computation of $Q(x)^{-1}$. For many applications, the cost J is known in advance of online implementation. In this case, $Q(x)^{-1}$ can be computed offline and in closed form. For example, consider the minimum-intervention specialization discussed in Section III. In this case, $Q = Q^{-1} = I_m$. If an application requires online computation of $Q(x)^{-1}$, then this typically has a worst-case complexity of $\mathcal{O}(m^3)$. For comparison, solving the quadratic program (18) using an interior-point method with an ϵ -tolerance typically has a complexity of $\mathcal{O}(m^3 \log(1/\epsilon))$ (e.g., [46, Chapter 3], [47, Chapter 6]). Thus, the closed-form control (10), (14), and (19)–(24) has a

computational-complexity advantage over the online solution of the quadratic program.

Note that if \mathcal{H} is compact, then (c) of Theorem 1 implies that u , μ , and λ are bounded on \mathcal{H} .

The next theorem is the main result on safety using this control.

Theorem 2. Consider (2), where (A1) is satisfied, and consider u given by (10), (14), and (19)–(24). Assume that h' is locally Lipschitz on \mathcal{H} , and for all $x \in \mathcal{B}$, $L_g h(x) \neq 0$. Let $x_0 \in \mathcal{S}$. Then, for all $t \in I(x_0)$, $x(t) \in \mathcal{S} \subseteq \mathcal{S}_s$.

Proof:

Since h' is locally Lipschitz on \mathcal{S} , it follows from (d) of Theorem 1 that u is locally Lipschitz on \mathcal{H} . Next, let $a \in \text{bd } \mathcal{H}$, which implies that $h(a) = 0$. Thus, (19)–(24) imply that

$$\begin{aligned} L_f h(a) + L_g h(a)u(a) &= L_f h(a) - L_g h(a)Q(a)^{-1}c(a) \\ &\quad + L_g h(a)Q(a)^{-1}L_g h(a)^T \lambda(a) \\ &= \begin{cases} 0, & a \in \Omega \\ \omega(a), & a \notin \Omega \end{cases} \\ &\geq 0. \end{aligned}$$

Hence, for all $x \in \text{bd } \mathcal{H}$, $L_f h(x) + L_g h(x)u(x) \geq 0$. Since, in addition, $x_0 \in \mathcal{S} \subseteq \mathcal{H}$, it follows from [43, Theorem 4.7] that for all $t \in I(x_0)$, $x(t) \in \mathcal{H}$, which implies that for all $t \in I(x_0)$, $h(x(t)) \geq 0$. Thus, (15), Proposition 2, and (11) imply that for all $t \in I(x_0)$, $b_{j,d_j-1}(x(t)) \geq 0$. Since, in addition, $x_0 \in \mathcal{S} \subseteq \mathcal{C}_j$, it follows from Lemma 2 that for all $t \in I(x_0)$, $x(t) \in \mathcal{C}_j$. Thus, for all $t \in I(x_0)$, $x(t) \in \mathcal{C}$, which implies that for all $t \in I(x_0)$, $x(t) \in \mathcal{S} = \mathcal{H} \cap \mathcal{C}$. ■

The control (10), (14), and (19)–(24) relies on the Lie derivatives $L_f h$ and $L_g h$, which can be expressed as

$$\begin{aligned} L_f h(x) &= \sum_{j=1}^{\ell} \beta_j(x) L_f b_{j,d_j-1}(x), \\ &= \sum_{j=1}^{\ell} \beta_j(x) \left[L_f^{d_j} h_j(x) \right. \\ &\quad \left. + \sum_{k=0}^{d_j-2} L_f^{k+1} \alpha_{j,d_j-2-k}(b_{j,d_j-2-k}(x)) \right], \\ L_g h(x) &= \sum_{j=1}^{\ell} \beta_j(x) L_g b_{j,d_j-1}(x) \\ &= \sum_{j=1}^{\ell} \beta_j(x) L_g L_f^{d_j-1} h_j(x), \end{aligned}$$

where

$$\beta_j(x) \triangleq \exp \rho(h(x) - b_{j,d_j-1}(x)).$$

It follows from (1) and (14) that $\sum_{j=1}^{\ell} \beta_j(x) = 1$, which implies that for each $x \in \mathbb{R}^n$, $L_f h(x)$ and $L_g h(x)$ are convex combinations of $L_f b_{1,d_1-1}(x), \dots, L_f b_{\ell,d_{\ell}-1}(x)$ and $L_g b_{1,d_1-1}(x), \dots, L_g b_{\ell,d_{\ell}-1}(x)$, respectively. Thus, if this

convex combination of $L_g b_{1,d_1-1}(x), \dots, L_g b_{\ell,d_\ell-1}(x)$ is not equal to the zero vector, then $L_g h(x) \neq 0$. The next result follows immediately from this observation and provides a sufficient condition such that $L_g h$ is nonzero on \mathcal{B} .

Proposition 5. Assume (A1) is satisfied, and assume for all $x \in \mathcal{B}$, $0 \notin \text{conv}\{L_g L_f^{d_1-1} h_1(x), \dots, L_g L_f^{d_\ell-1} h_\ell(x)\}$. Then, for all $x \in \mathcal{B}$, $L_g h(x) \neq 0$.

For certain applications, Proposition 5 can be used to verify that $L_g h$ is nonzero on \mathcal{B} . For example, if the corresponding elements of $L_g L_f^{d_1-1} h_1(x), \dots, L_g L_f^{d_\ell-1} h_\ell(x)$ have the same sign, then Proposition 5 implies that $L_g h$ is nonzero on \mathcal{B} . Although Proposition 5 provides a sufficient condition such that $L_g h$ is nonzero on \mathcal{B} , we note that this condition is not necessary.

Next, we present an example to demonstrate the optimal soft-minimum R-CBF control (10), (14), and (19)–(24).

Example 1. Consider the nonholonomic ground robot modeled by (2), where

$$f(x) = \begin{bmatrix} v \cos \theta \\ v \sin \theta \\ 0 \\ 0 \end{bmatrix}, g(x) = \begin{bmatrix} 0 & 0 \\ 0 & 0 \\ 1 & 0 \\ 0 & 1 \end{bmatrix}, x = \begin{bmatrix} q_x \\ q_y \\ v \\ \theta \end{bmatrix}, u = \begin{bmatrix} u_1 \\ u_2 \end{bmatrix},$$

and $q \triangleq [q_x \ q_y]^T$ is the robot's position in an orthogonal coordinate system, v is the speed, and θ is the direction of the velocity vector (i.e., the angle from $[1 \ 0]^T$ to $[\dot{q}_x \ \dot{q}_y]^T$).

Consider the map shown in Figure 3, which has 6 obstacles and a wall. For $j \in \{1, \dots, 6\}$, the area outside the j th obstacle is modeled as the zero-superlevel set of

$$h_j(x) = \left\| \begin{bmatrix} a_{x,j}(q_x - b_{x,j}) \\ a_{y,j}(q_y - b_{y,j}) \end{bmatrix} \right\|_p - c_j, \quad (25)$$

where $b_{x,j}, b_{y,j}, a_{x,j}, a_{y,j}, c_j, p > 0$ specify the location and dimensions of the j th obstacle. Similarly, the area inside the wall is modeled as the zero-superlevel set of

$$h_7(x) = c_7 - \left\| \begin{bmatrix} a_{x,7} q_x \\ a_{y,7} q_y \end{bmatrix} \right\|_p, \quad (26)$$

where $a_{x,7}, a_{y,7}, c_7, p > 0$ specify the dimension of the space inside the wall. The bounds on speed v are modeled as the zero-superlevel sets of

$$h_8(x) = 9 - v, \quad h_9(x) = v + 1. \quad (27)$$

The safe set \mathcal{S}_s is given by (8) where $\ell = 9$. The projection of \mathcal{S}_s onto the q_x - q_y plane is shown in Figure 3. Note that for all $x \in \mathcal{S}_s$, the speed satisfies $v \in [-1, 9]$. We also note that (A1) is satisfied with $d_1 = d_2 = \dots = d_7 = 2$ and $d_8 = d_9 = 1$.

Let $q_d = [q_{d,x} \ q_{d,y}]^T \in \mathbb{R}^2$ be the goal location, that is, the desired location for q . Then, consider the desired control

$$u_d(x) \triangleq \begin{bmatrix} u_{d_1}(x) \\ u_{d_2}(x) \end{bmatrix}, \quad (28)$$

where $u_{d_1}, u_{d_2}, \psi: \mathbb{R}^4 \rightarrow \mathbb{R}$ are

$$u_{d_1}(x) \triangleq -(k_1 + k_3)v + (1 + k_1 k_3) \|q - q_d\|_2 \cos \psi(x) + k_1 (k_2 \|q - q_d\|_2 + v) \sin^2 \psi(x), \quad (29)$$

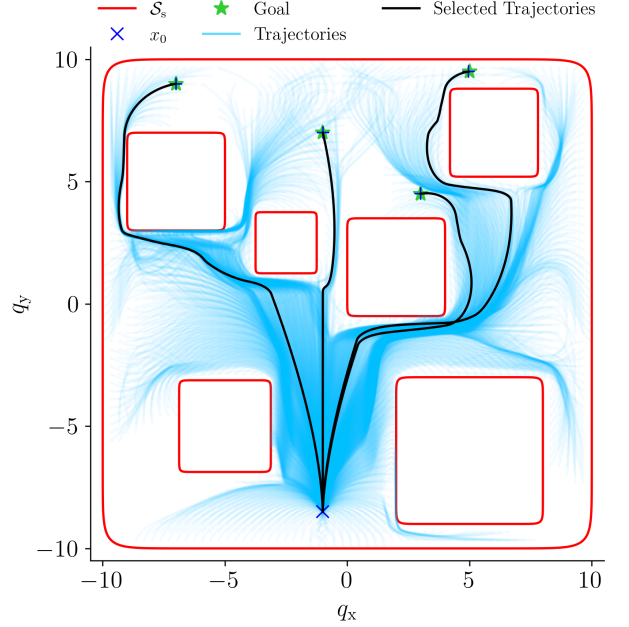


FIGURE 3. Safe set \mathcal{S}_s , and 2,500 closed-loop trajectories using the control (10), (14), and (19)–(24).

$$u_{d_2}(x) \triangleq \left(k_2 + \frac{v}{\|q - q_d\|_2} \right) \sin \psi(x), \quad (30)$$

$$\psi(x) \triangleq \text{atan2}(q_y - q_{d,y}, q_x - q_{d,x}) - \theta + \pi, \quad (31)$$

and $k_1 = 0.2, k_2 = 1$, and $k_3 = 2$. Note that the desired control is designed using a process similar to [48, pp. 30–31], and it drives $[q_x \ q_y]^T$ to q_d but does not account for safety.

We consider the cost (9), where $Q(x) = I_2$ and $c(x) = -u_d(x)$. Thus, the minimizer of (9) is equal to the minimizer $u_d(x)$ of the minimum-intervention cost $\|u - u_d(x)\|_2^2$.

We implement the control (10), (14), and (19)–(24) with $\rho = 10$, $\gamma = 10^{24}$, $\alpha_{1,0}(h) = \dots = \alpha_{7,0}(h) = 10h$, and $\alpha(h) = 0.5h$. In this example, we use large γ (i.e., $\gamma = 10^{24}$) to enforce the constraint (18b) without relying on the slack variable (i.e., $\mu \approx 0$). Smaller γ can also be used to obtain more aggressive behavior, where the closed-loop response gets closer to the obstacles or speed limits. However, the choice of $\alpha_{j,0}$ in this example is relatively aggressive (i.e., $\alpha'_{j,0} = 10$). Hence, if smaller γ is used, then $\alpha'_{j,0}$ should be decreased to limit the magnitude of the time derivative of the control signals. For sample-data implementation, the control is updated at 40 Hz.

Figure 3 shows 2,500 closed-loop trajectories for $x_0 = [-1 \ -8.5 \ 0 \ \pi/2]^T$ and randomly distributed goal locations. For each case, all safety constraints are satisfied along the closed-loop trajectory. Certain goal locations in \mathcal{S}_s cannot be reached, which is expected because the desired control (28)–(31) does not account for any safety constraints. In other words, (28)–(31) is not designed using knowledge of the obstacles or speed limits. For this example, increasing the gains k_1, k_2, k_3 in the desired control (28)–(31) enlarges

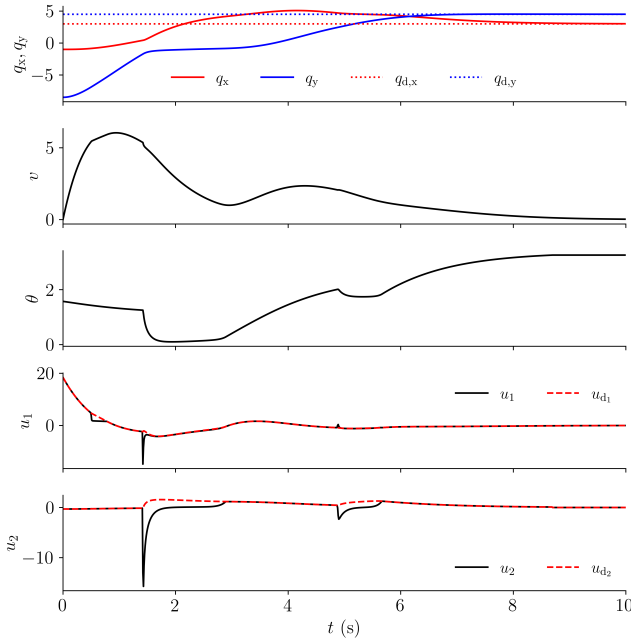


FIGURE 4. q_x, q_y, v, θ, u and u_d for $q_d = [3 \ 4.5]^T$.

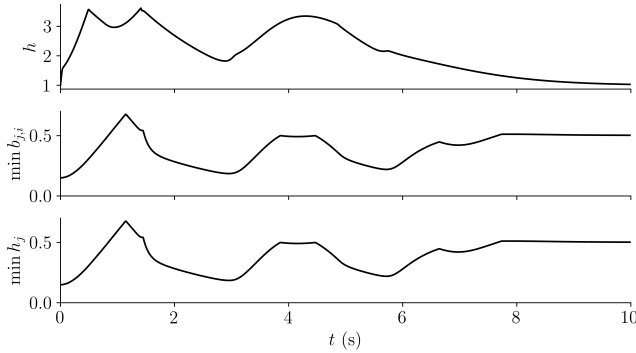


FIGURE 5. $h, \min b_{j,i}$, and $\min h_j$ for $q_d = [3 \ 4.5]^T$.

the set of reachable goal locations. Alternatively, designing a desired control that uses information about the obstacles can also enlarge the set of reachable goal locations.

Figure 3 also highlights the closed-loop trajectories for 4 selected goal locations: $q_d = [3 \ 4.5]^T$, $q_d = [-7 \ 9]^T$, $q_d = [5 \ 9.5]^T$, and $q_d = [-1 \ 7]^T$. Figures 4 and 5 show the trajectories of the relevant signals for the case where $q_d = [3 \ 4.5]^T$. Figure 5 shows that $h, \min b_{j,i}$, and $\min h_j$ are positive for all time, which implies that the trajectory remains in $\mathcal{S} \subseteq \mathcal{S}_s$. The control u deviates significantly from u_d at $t = 1.4$ s. This occurs, in large part, because the desired control (28)–(31) does not account for the obstacles or speed limits. This effect can be mitigated by using a less aggressive choice for $\alpha_{j,0}$.

For comparison, we present simulation results with an alternative control approach that uses multiple higher-order CBFs (HOCBFs). Specifically, the control is generated from a quadratic program that has multiple constraints—one for

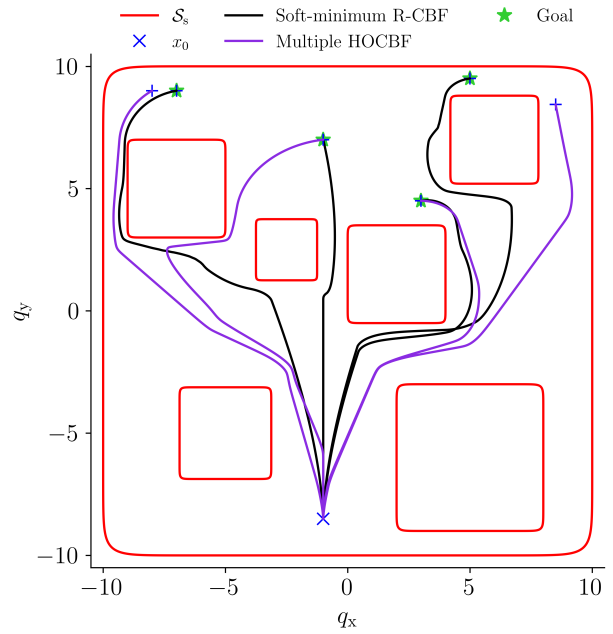


FIGURE 6. Closed-loop trajectories for 4 goal locations using the soft-minimum R-CBF method and the multiple-HOCBF method.

each HOCBF (e.g., see [49]). In this example, h_1, h_2, \dots, h_9 are each used to form individual CBF-based constraints for a quadratic program that uses the minimum-intervention cost. All parameters are the same as in the above soft-minimum R-CBF implementation. Out of the 2,500 random goal locations, the multiple-HOCBF approach resulted in an infeasible quadratic program along 103 of the solution trajectories. Some of these feasibility violations are minor and did not result in safety violations; however, this illustrates that feasibility is not generally guaranteed using multiple HOCBF-based constraints. Example 4 in the next section demonstrates that this issue with multiple-HOCBF methods is exacerbated when there are also input constraints.

Figure 6 shows 4 solution trajectories using the soft-minimum R-CBF method and using the multiple-HOCBF method. Two of the trajectories shown are selected from the 103 where the multiple-HOCBF method is infeasible. For these 2 cases, the trajectory ends at the time instant when the optimization is infeasible.

Simulations are implemented in Python on a laptop computer with an Intel Core i9-9880H CPU¹. For the multiple-HOCBF approach, the quadratic program is solved using the OptNet package [50]. The average computation time for the soft-minimum R-CBF method is 2 ms per iteration, while it is 30 ms for the multiple-HOCBF approach, which illustrates the computational benefit of the soft-minimum R-CBF method. In fact, the computation time for the soft-minimum R-CBF method is negligible if $L_f h$ and $L_g h$ are calculated analytically offline rather than in real time. \triangle

¹https://github.com/pedramrabiee/hocbf_composition

VI. Safety with Input Constraints

This section presents a closed-form optimal control that not only guarantees safety but also respects specified input constraints (e.g., actuator limits). We reconsider the system (2), safe set (8), and cost (9). Next, let $\phi_1, \dots, \phi_{\ell_u} : \mathbb{R}^m \rightarrow \mathbb{R}$ be continuously differentiable, and define the set of admissible controls

$$\mathcal{U} \triangleq \{u \in \mathbb{R}^m : \phi_1(u) \geq 0, \dots, \phi_{\ell_u}(u) \geq 0\} \subseteq \mathbb{R}^m. \quad (32)$$

We assume that for all $u \in \mathcal{U}$ and all $\kappa \in \{1, 2, \dots, \ell_u\}$, $\phi'_\kappa(u) \neq 0$. Unless otherwise stated, all statements in this section that involve the subscript κ are for all $\kappa \in \{1, 2, \dots, \ell_u\}$.

The control objective is to design a full-state feedback control such that for all $t \in I(x_0)$, $J(x(t), u(t))$ is minimized subject to the safety constraint that $x(t) \in \mathcal{S}_s$ and the input constraint that $u(t) \in \mathcal{U}$.

Before presenting an approach to this general problem, the next example considers a special case where there is one safety constraint that is relative degree one and one input constraint. The example illustrates the 3 key elements used to address safety with input constraints: (1) control dynamics to transform the input constraint into a controller-state constraint; (2) soft-minimum R-CBF to compose the safety constraint and controller-state constraint; and (3) a desired surrogate control (i.e., desired input to the control dynamics).

Example 2. We consider a scenario, where there is one safety constraint (i.e., $\ell = 1$) that is relative degree one (i.e., $d_1 = 1$) and one input constraint (i.e., $\ell_u = 1$). Thus, the safety constraint is described by the zero-superlevel set of h_1 and the input constraint is described by the zero-superlevel set of ϕ_1 .

First, consider a control u generated by the first-order linear time-invariant (LTI) control dynamics

$$\dot{u}(t) = -au(t) + a\hat{u}(x(t), u(t)), \quad (33)$$

where $a > 0$, $u(0) \in \mathbb{R}^m$ is the initial condition, and $\hat{u} : \mathbb{R}^n \times \mathbb{R}^m \rightarrow \mathbb{R}^m$ is the *surrogate control* (i.e., input to the control dynamics). The cascade of (2) and (33) is

$$\dot{\hat{x}} = \hat{f}(\hat{x}) + \hat{g}(\hat{x})\hat{u}, \quad (34)$$

where

$$\hat{x} \triangleq \begin{bmatrix} x \\ u \end{bmatrix}, \quad \hat{f}(\hat{x}) \triangleq \begin{bmatrix} f(x) + g(x)u \\ -au \end{bmatrix}, \quad \hat{g}(\hat{x}) \triangleq \begin{bmatrix} 0 \\ a \end{bmatrix}. \quad (35)$$

Define

$$\hat{\mathcal{S}}_s \triangleq \mathcal{S}_s \times \mathcal{U},$$

which is the set of system-and-controller states \hat{x} such that the safety constraint is satisfied (i.e., $h_1(x) \geq 0$) and the input constraint is satisfied (i.e., $\phi_1(u) \geq 0$). Define

$$\hat{h}_1(\hat{x}) \triangleq h_1(x), \quad \hat{h}_2(\hat{x}) \triangleq \phi_1(u),$$

and for $j \in \{1, 2\}$, the zero-superlevel sets are

$$\hat{\mathcal{C}}_{j,0} \triangleq \{\hat{x} \in \mathbb{R}^{n+m} : \hat{h}_j(\hat{x}) \geq 0\}.$$

Thus, $\hat{\mathcal{S}}_s = \hat{\mathcal{C}} \triangleq \hat{\mathcal{C}}_{1,0} \cap \hat{\mathcal{C}}_{2,0}$, which demonstrates that the control dynamics (33) transforms the input constraint into a

controller-state constraint. However, \hat{h}_1 and \hat{h}_2 have different relative degrees with respect to the cascade (34) and (35); specifically, the relative degrees are $\hat{d}_1 = 2$ and $\hat{d}_2 = 1$. Thus, the introducing control dynamics also increases the relative degree of the original safety constraint. Nevertheless, the soft-minimum R-CBF construction can be used to construct a single R-CBF from \hat{h}_1 and \hat{h}_2 .

To use the soft-minimum R-CBF to compose \hat{h}_1 (safety constraint) and \hat{h}_2 (controller-state constraint), we follow the steps in Section IV but where each symbol is replaced by that symbol with a hat (i.e., $\hat{\cdot}$). Specifically, we define

$$\begin{aligned} \hat{b}_{1,0}(\hat{x}) &\triangleq \hat{h}_1(\hat{x}), & \hat{b}_{2,0}(\hat{x}) &\triangleq \hat{h}_2(\hat{x}), \\ \hat{b}_{1,1}(\hat{x}) &\triangleq L_{\hat{f}}\hat{h}_1(\hat{x}) + \hat{\alpha}_{1,0}(\hat{h}_1(\hat{x})) \end{aligned}$$

where $\hat{\alpha}_{1,0} : \mathbb{R} \rightarrow \mathbb{R}$ is a locally Lipschitz extended class- \mathcal{K} function. Then, the composite soft-minimum R-CBF is

$$\hat{h}(\hat{x}) \triangleq \text{softmin}_\rho(\hat{b}_{1,1}(\hat{x}), \hat{b}_{2,0}(\hat{x})),$$

and its zero-superlevel set is

$$\hat{\mathcal{H}} \triangleq \{\hat{x} \in \mathbb{R}^{n+m} : \hat{h}(\hat{x}) \geq 0\}.$$

Next, Lemma 1 implies that \hat{h} is an R-CBF if for all $x \in \hat{\mathcal{B}} \triangleq \{x \in \text{bd } \hat{\mathcal{H}} : L_{\hat{f}}\hat{h}(\hat{x}) \leq 0\}$, $L_{\hat{g}}\hat{h}(\hat{x}) \neq 0$. Thus, we aim to use \hat{h} to construct a closed-form optimal surrogate control \hat{u} such that $\hat{x}(t) \in \hat{\mathcal{S}} \triangleq \hat{\mathcal{H}} \cap \hat{\mathcal{C}}$, which implies that the safety and input constraints are satisfied. However, we cannot directly apply the process in Section V because the cost J given by (9) is a function of u rather than \hat{u} .

To address this issue, we define the *desired surrogate control*

$$\hat{u}_d(\hat{x}) \triangleq u + \frac{1}{a} \left(u'_d(x) (f(x) + g(x)u) + \sigma_0 (u_d(x) - u) \right), \quad (36)$$

where $\sigma_0 > 0$ and $u_d(x) \triangleq -Q(x)^{-1}c(x)$, which is the unconstrained minimizer of (9). We note that \hat{u}_d is a feedback linearizing input for the cascade (34) and (35); it makes the error between the control u and the desired control u_d satisfy asymptotically stable LTI dynamics. More specifically, if $\hat{u} = \hat{u}_d$, then substituting (36) into (33) yields

$$\frac{d}{dt}[u(t) - u_d(x(t))] + \sigma_0[u(t) - u_d(x(t))] = 0.$$

Hence, the desired surrogate control (36) yields u that converges exponentially to u_d , which is the minimizer of J . Next, we consider the *surrogate cost function*

$$\hat{J}(\hat{x}, \hat{u}) \triangleq \frac{1}{2} \|\hat{u} - \hat{u}_d(\hat{x})\|_2^2,$$

and we can obtain an optimal surrogate control \hat{u} that satisfies safety and input constraints by solving the quadratic program (18), where h , $L_{\hat{f}}h$, $L_{\hat{g}}h$, and J are replaced by \hat{h} , $L_{\hat{f}}\hat{h}$, $L_{\hat{g}}\hat{h}$, and \hat{J} . This results in a closed-form for \hat{u} that is given by (19)–(24), where $Q = I_m$, $c = -\hat{u}_d$, and h , $L_{\hat{f}}h$, and $L_{\hat{g}}h$ are replaced by \hat{h} , $L_{\hat{f}}\hat{h}$, and $L_{\hat{g}}\hat{h}$. \triangleleft

The remainder of this section formalizes and generalizes the approach demonstrated in Example 2. We generalize to an arbitrary number of safety constraints with potentially different relative degrees, an arbitrary number of input constraints, and a general class of nonlinear control dynamics. Moreover, we analyze the properties of this approach.

A. Control Dynamics to Transform Input Constraints into Controller-State Constraints

To address safety with input constraints, consider a control u that satisfies

$$\dot{x}_c(t) = f_c(x_c(t)) + g_c(x_c(t))\hat{u}(x(t), x_c(t)), \quad (37)$$

$$u(t) = h_c(x_c(t)), \quad (38)$$

where $x_c(t) \in \mathbb{R}^{n_c}$ is the controller state; $x_c(0) = x_{c0} \in \mathbb{R}^{n_c}$ is the initial condition; $f_c : \mathbb{R}^{n_c} \rightarrow \mathbb{R}^{n_c}$, $g_c : \mathbb{R}^{n_c} \rightarrow \mathbb{R}^{n_c \times m}$, and $h_c : \mathbb{R}^{n_c} \rightarrow \mathbb{R}^m$ are locally Lipschitz on \mathbb{R}^{n_c} ; and $\hat{u} : \mathbb{R}^{n+n_c} \rightarrow \mathbb{R}^m$ is the *surrogate control* (i.e., input to the control dynamics), which is given by the closed-form solution to a quadratic program presented later in this section.

Define

$$\mathcal{S}_c \triangleq \{x_c \in \mathbb{R}^{n_c} : h_c(x_c) \in \mathcal{U}\}, \quad (39)$$

which is the set of controller states such that the control is in \mathcal{U} . Thus, the control dynamics (37) and (38) transforms the input constraint (i.e., $u(t) \in \mathcal{U}$) into a constraint on the controller state (i.e., $x_c(t) \in \mathcal{S}_c$).

Next, the cascade of (2), (37), and (38) is given by

$$\dot{\hat{x}} = \hat{f}(\hat{x}) + \hat{g}(\hat{x})\hat{u}, \quad (40)$$

where

$$\hat{x} \triangleq \begin{bmatrix} x \\ x_c \end{bmatrix}, \quad \hat{f}(\hat{x}) \triangleq \begin{bmatrix} f(x) + g(x)h_c(x_c) \\ f_c(x_c) \end{bmatrix}, \quad (41)$$

$$\hat{g}(\hat{x}) \triangleq \begin{bmatrix} 0 \\ g_c(x_c) \end{bmatrix}, \quad \hat{x}_0 \triangleq \begin{bmatrix} x_0 \\ x_{c0} \end{bmatrix}, \quad (42)$$

and $\hat{n} \triangleq n + n_c$. Define

$$\hat{\mathcal{S}}_s \triangleq \mathcal{S}_s \times \mathcal{S}_c, \quad (43)$$

which is the set of cascade states \hat{x} such that the safety constraint (i.e., $x(t) \in \mathcal{S}_s$) and the input constraint (i.e., $u(t) \in \mathcal{U}$) are satisfied. The next result summarizes this property. The proof is in Appendix A.

Proposition 6. Assume that for all $t \in I(\hat{x}_0)$, $\hat{x}(t) \in \hat{\mathcal{S}}_s$. Then, for all $t \in I(\hat{x}_0)$, $x(t) \in \mathcal{S}_s$ and $u(t) \in \mathcal{U}$.

The functions f_c , g_c and h_c are selected such that the following conditions hold:

- (C1) There exists a positive integer d_c such that for all $x_c \in \mathbb{R}^{n_c}$ and all $i \in \{0, 1, \dots, d_c - 2\}$, $L_{g_c} L_{f_c}^i h_c(x_c) = 0$; and for all $x_c \in \mathbb{R}^{n_c}$, $L_{g_c} L_{f_c}^{d_c-1} h_c(x_c)$ is nonsingular.
- (C2) There exists a positive integer ζ such that for all $x_c \in \mathbb{R}^{n_c}$ and all $i \in \{0, 1, \dots, \zeta - 2\}$, $L_{g_c} L_{f_c}^i \phi_\kappa(h_c(x_c)) = 0$; and for all $x_c \in \mathcal{S}_c$, $L_{g_c} L_{f_c}^{\zeta-1} \phi_\kappa(h_c(x_c)) \neq 0$.

The following example provides one construction for f_c , g_c , and h_c such that (C1) and (C2) are satisfied. In particular, the example demonstrates that (C1) and (C2) are satisfied by any LTI construction of (37) and (38) where the first Markov parameter is nonsingular.

Example 3. Let

$$f_c(x_c) = A_c x_c, \quad g_c(x_c) = B_c, \quad h_c(x_c) = C_c x_c,$$

where $A_c \in \mathbb{R}^{n_c \times n_c}$, $B_c \in \mathbb{R}^{n_c \times m}$, $C_c \in \mathbb{R}^{m \times n_c}$, and $C_c B_c$ is nonsingular. Note that $L_{g_c} h_c(x_c) = C_c B_c$, which implies that (C1) is satisfied with $d_c = 1$. Next, note that $L_{g_c} \phi_\kappa(h_c(x_c)) = \phi'_\kappa(h_c(x_c)) C_c B_c$. Since $C_c B_c$ is nonsingular and for all $x_c \in \mathcal{S}_c$, $\phi'_\kappa(h_c(x_c)) \neq 0$, it follows that (C2) is satisfied with $\zeta = 1$. Thus, any LTI controller with $C_c B_c$ nonsingular satisfies (C1) and (C2). In fact, any LTI controller where the first nonzero Markov parameter is nonsingular satisfies (C1) and (C2).

The control dynamics (33) used in Example 2 is a special case where $A_c = -aI_{n_c}$, $B_c = aI_{n_c}$, $C_c = I_{n_c}$, which results in low-pass control dynamics. \triangle

Next, we examine the relative degree of each safety and input constraint function with respect to the cascade (40)–(42). Unless otherwise stated, all statements in this section that involve the subscript \hat{j} are for all $\hat{j} \in \{1, 2, \dots, \hat{\ell}\}$, where $\hat{\ell} \triangleq \ell + \ell_u$. Let $\hat{h}_{\hat{j}} : \mathbb{R}^{\hat{n}} \rightarrow \mathbb{R}$ be defined by

$$\hat{h}_{\hat{j}}(\hat{x}) \triangleq \begin{cases} h_{\hat{j}}(x), & \text{if } \hat{j} \in \{1, 2, \dots, \ell\}, \\ \phi_{\hat{j}-\ell}(h_c(x_c)), & \text{if } \hat{j} \in \{\ell + 1, \ell + 2, \dots, \ell + \ell_u\}, \end{cases} \quad (44)$$

and define

$$\hat{d}_{\hat{j}} \triangleq \begin{cases} d_{\hat{j}} + d_c, & \text{if } \hat{j} \in \{1, 2, \dots, \ell\}, \\ \zeta, & \text{if } \hat{j} \in \{\ell + 1, \ell + 2, \dots, \ell + \ell_u\}. \end{cases} \quad (45)$$

The following result demonstrates that $\hat{h}_{\hat{j}}$ has well-defined relative degree $\hat{d}_{\hat{j}}$ with respect to the cascade (40)–(42) on $\hat{\mathcal{S}}_s$; however, relative degrees $\hat{d}_1, \dots, \hat{d}_{\hat{\ell}}$ are not all equal. The proof is in Appendix A.

Proposition 7. Consider (2), where (A1) is satisfied, and consider (37) and (38), where (C1) and (C2) are satisfied. Then, for all $\hat{x} \in \mathbb{R}^{\hat{n}}$, all $\hat{j} \in \{1, 2, \dots, \hat{\ell}\}$, and all $i \in \{0, 1, \dots, \hat{d}_{\hat{j}} - 2\}$, $L_{\hat{g}} L_{\hat{f}}^i \hat{h}_{\hat{j}}(\hat{x}) = 0$; and for all $\hat{x} \in \hat{\mathcal{S}}_s$ and all $\hat{j} \in \{1, 2, \dots, \hat{\ell}\}$, $L_{\hat{g}} L_{\hat{f}}^{\hat{d}_{\hat{j}}-1} \hat{h}_{\hat{j}}(\hat{x}) \neq 0$.

Proposition 7 illustrates that the control dynamics (37) and (38) increase the relative degree of each system-state constraint (i.e., safety constraint) by d_c . In general, it is desirable to design (37) and (38) such that d_c is low, which tends to limit lag. Example 3 demonstrates that it is always possible to design (37) and (38) such that $d_c = 1$.

B. Composite Soft-Minimum R-CBF

Proposition 7 implies that the cascade (40)–(42) satisfy (A1), where f , g , x , \mathcal{S}_c , ℓ , j , h_j , and d_j are replaced by \hat{f} , \hat{g} , \hat{x} , $\hat{\mathcal{S}}_c$, $\hat{\ell}$, \hat{j} , $\hat{h}_{\hat{j}}$, and $\hat{d}_{\hat{j}}$. Thus, the composite soft-

minimum R-CBF construction in Section IV can be applied to the cascade (40)–(42) to construct a single R-CBF from $\hat{h}_1, \dots, \hat{h}_{\hat{d}_j}$, which do not all have the same relative degree. Note that $\hat{h}_1, \dots, \hat{h}_{\hat{d}_j}$ describe the set $\hat{\mathcal{S}}_s = \mathcal{S}_s \times \mathcal{S}_c$ that combines the safe set \mathcal{S}_s and the set \mathcal{S}_c of controller states such that the control is in \mathcal{U} . Thus, the soft-minimum R-CBF can address safety constraints and input constraints.

We construct this soft-minimum R-CBF by following (10)–(17) in Section IV but where each symbol is replaced by that symbol with a hat (i.e., $\hat{\cdot}$). Specifically, let $\hat{b}_{j,0}(\hat{x}) \triangleq \hat{h}_j(\hat{x})$. For $i \in \{0, 1, \dots, \hat{d}_j - 2\}$, let $\hat{\alpha}_{j,i}: \mathbb{R} \rightarrow \mathbb{R}$ be a locally Lipschitz extended class- \mathcal{K} function, and consider $\hat{b}_{j,i+1}: \mathbb{R}^{\hat{n}} \rightarrow \mathbb{R}$ defined by

$$\hat{b}_{j,i+1}(\hat{x}) \triangleq L_f \hat{b}_{j,i}(\hat{x}) + \hat{\alpha}_{j,i}(\hat{b}_{j,i}(\hat{x})). \quad (46)$$

For $i \in \{0, \dots, \hat{d}_j - 1\}$, define

$$\hat{\mathcal{C}}_{j,i} \triangleq \{\hat{x} \in \mathbb{R}^{\hat{n}}: \hat{b}_{j,i}(\hat{x}) \geq 0\}.$$

Next, define

$$\hat{\mathcal{C}}_j \triangleq \begin{cases} \hat{\mathcal{C}}_{j,0}, & \hat{d}_j = 1, \\ \bigcap_{i=0}^{\hat{d}_j-2} \hat{\mathcal{C}}_{j,i}, & \hat{d}_j > 1, \end{cases}$$

and

$$\hat{\mathcal{C}} \triangleq \bigcap_{j=1}^{\hat{\ell}} \hat{\mathcal{C}}_j.$$

Let $\rho > 0$, and consider $\hat{h}: \mathbb{R}^{\hat{n}} \rightarrow \mathbb{R}$ defined by

$$\hat{h}(\hat{x}) \triangleq \text{softmin}_{\rho} \left(\hat{b}_{1,\hat{d}_1-1}(\hat{x}), \hat{b}_{2,\hat{d}_2-1}(\hat{x}), \dots, \hat{b}_{\hat{\ell},\hat{d}_{\hat{\ell}}-1}(\hat{x}) \right). \quad (47)$$

Furthermore, define

$$\hat{\mathcal{H}} \triangleq \{\hat{x} \in \mathbb{R}^{\hat{n}}: \hat{h}(\hat{x}) \geq 0\}, \quad \hat{\mathcal{S}} \triangleq \hat{\mathcal{H}} \cap \hat{\mathcal{C}}, \\ \hat{\mathcal{B}} \triangleq \{\hat{x} \in \text{bd } \hat{\mathcal{H}}: L_f \hat{h}(\hat{x}) \leq 0\}.$$

Lemma 1 implies that if $L_{\hat{g}} \hat{h}$ is nonzero on $\hat{\mathcal{B}}$, then \hat{h} is an R-CBF. The next result is a corollary of Proposition 3, which is obtained by applying Proposition 3 to the cascade (40)–(42).

Corollary 1. Consider (2), where (A1) is satisfied, and consider (37) and (38), where (C1) and (C2) are satisfied. Assume that \hat{h}' is locally Lipschitz on $\hat{\mathcal{H}}$, and for all $\hat{x} \in \hat{\mathcal{B}}$, $L_{\hat{g}} \hat{h}(\hat{x}) \neq 0$. Then, $\hat{\mathcal{S}}$ is control forward invariant.

Corollary 1 provides conditions under which $\hat{\mathcal{S}} \subseteq \hat{\mathcal{S}}_s$ is control forward invariant. In this case, \hat{h} is an R-CBF that can be used to generate a control such that for all $t \in I(\hat{x}_0)$, $\hat{x}(t) \in \hat{\mathcal{S}} \subseteq \hat{\mathcal{S}}_s$, which implies that $x(t) \in \mathcal{S}_s$ and $u(t) \in \mathcal{U}$.

C. Desired Surrogate Control

Although \hat{h} is an R-CBF, we cannot directly apply a quadratic program similar to (18) because the cost J given by (9) is a function of u rather than the surrogate control \hat{u} . Consider the *desired control* $u_d: \mathbb{R}^{\hat{n}} \rightarrow \mathbb{R}^m$ defined by

$$u_d(\hat{x}) \triangleq -Q(x)^{-1}c(x), \quad (48)$$

which is the minimizer of (9). Next, consider the *desired surrogate control* $\hat{u}_d: \mathbb{R}^{\hat{n}} \rightarrow \mathbb{R}^m$ defined by

$$\hat{u}_d(\hat{x}) \triangleq \left(L_{g_c} L_{f_c}^{d_c-1} h_c(x_c) \right)^{-1} \left(L_{f_c}^{d_c} u_d(\hat{x}) - L_{f_c}^{d_c} h_c(x_c) \right. \\ \left. + \sum_{i=0}^{d_c-1} \sigma_i \left(L_{f_c}^i u_d(\hat{x}) - L_{f_c}^i h_c(x_c) \right) \right), \quad (49)$$

where $\sigma_0, \sigma_1, \dots, \sigma_{d_c-1} > 0$ are selected such that

$$\sigma(s) \triangleq s^{d_c} + \sigma_{d_c-1} s^{d_c-1} + \sigma_{d_c-2} s^{d_c-2} + \dots + \sigma_1 s + \sigma_0$$

has all its roots in the open left-hand complex plane.

The desired surrogate control (49) is the generalization of (36) to any f_c, g_c, h_c , and d_c that satisfy (C1) and (C2). In particular, (49) is a feedback linearizing input for the cascade (40)–(42); it makes the error between u and u_d satisfy asymptotically stable LTI dynamics. The next result formalizes this fact. The proof is in Appendix A.

Proposition 8. Consider (2), where (A1) is satisfied, and consider (37) and (38), where (C1) is satisfied and $\hat{u}(\hat{x}) = \hat{u}_d(\hat{x})$. Then, the following statements hold:

(a) The error $u - u_d(\hat{x})$ satisfies

$$\frac{d^{d_c}}{dt^{d_c}} [u(t) - u_d(\hat{x}(t))] \\ + \sum_{i=0}^{d_c-1} \sigma_i \frac{d^i}{dt^i} [u(t) - u_d(\hat{x}(t))] = 0. \quad (50)$$

(b) For all $\hat{x}_0 \in \mathbb{R}^{\hat{n}}$, $\lim_{t \rightarrow \infty} [u(t) - u_d(\hat{x}(t))] = 0$ exponentially.

(c) Assume that Q is bounded. Then, for all $\hat{x}_0 \in \mathbb{R}^{\hat{n}}$,

$$\lim_{t \rightarrow \infty} [J(x(t), u(t)) - J(x(t), u_d(\hat{x}(t)))] = 0.$$

(d) Let $x_0 \in \mathbb{R}^n$, and assume $x_{c0} \in \mathbb{R}^{m_c}$ is such that for $i \in \{0, 1, \dots, d_c - 1\}$, $L_{f_c}^i h_c(x_{c0}) = L_{f_c}^i u_d(\hat{x}_0)$. Then, $u(t) \equiv u_d(\hat{x}(t))$.

Proposition 8 implies that the control dynamics (37) and (38) with $\hat{u} = \hat{u}_d$ yields a control u that converges exponentially to the desired control u_d , which is the minimizer of J . Thus, we introduce the surrogate cost function $\hat{J}: \mathbb{R}^{\hat{n}} \times \mathbb{R}^m \rightarrow \mathbb{R}$ defined by

$$\hat{J}(\hat{x}, \hat{u}) \triangleq \frac{1}{2} \|\hat{u} - \hat{u}_d(\hat{x})\|_2^2. \quad (51)$$

Note that if \hat{u} equals the minimizer \hat{u}_d of \hat{J} , then u converges exponentially to the minimizer u_d of J . In the next subsection, we design a control \hat{u} with the goal that for all $t \in I(\hat{x}_0)$, $\hat{J}(\hat{x}(t), \hat{u}(\hat{x}(t)))$ is minimized subject to the constraint that $\hat{x}(t) \in \hat{\mathcal{S}} \subseteq \hat{\mathcal{S}}_s$, which implies that the safety constraints and the input constraints are satisfied.

D. Closed-Form Optimal and Safe Control with Input Constraints

Let $\gamma > 0$, and let $\alpha: \mathbb{R} \rightarrow \mathbb{R}$ be a locally Lipschitz nondecreasing function such that $\alpha(0) = 0$. For all $\hat{x} \in \mathbb{R}^{\hat{n}}$,

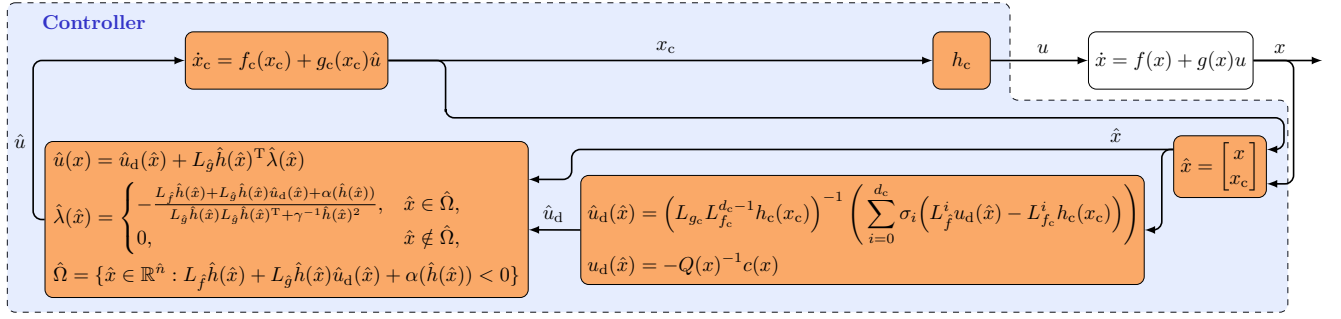


FIGURE 7. Closed-form optimal and safe control with input constraints. Control uses the composite soft-minimum R-CBF \hat{h} to guarantee safety and input constraints are satisfied. Control minimizes cost subject to safety and input constraints.

consider the control given by

$$\left(\hat{u}(\hat{x}), \hat{\mu}(\hat{x})\right) \triangleq \underset{\hat{u} \in \mathbb{R}^m, \hat{\mu} \in \mathbb{R}}{\operatorname{argmin}} \quad \hat{J}(\hat{x}, \hat{u}) + \frac{1}{2}\gamma\hat{\mu}^2 \quad (52a)$$

subject to

$$L_{\hat{f}}\hat{h}(\hat{x}) + L_{\hat{g}}\hat{h}(\hat{x})\hat{u} + \alpha(\hat{h}(\hat{x})) + \hat{\mu}\hat{h}(\hat{x}) \geq 0. \quad (52b)$$

Proposition 4 applied to the cascade (40)–(42) implies that if $L_{\hat{g}}\hat{h}$ is nonzero on $\hat{\mathcal{B}}$, then the quadratic program (52) is feasible on \mathbb{R}^n . The following result provides a closed-form solution for the control \hat{u} that satisfies (52). This result is a corollary of Theorem 1, which is obtained by applying Theorem 1 to the constrained optimization (52) and cascade (40)–(42).

Corollary 2. Assume that for all $\hat{x} \in \hat{\mathcal{B}}$, $L_{\hat{g}}\hat{h}(\hat{x}) \neq 0$. Then,

$$\hat{u}(\hat{x}) = \hat{u}_d(\hat{x}) + L_{\hat{g}}\hat{h}(\hat{x})^T \hat{\lambda}(\hat{x}) \quad (53)$$

where

$$\hat{\lambda}(\hat{x}) = \begin{cases} -\frac{L_{\hat{f}}\hat{h}(\hat{x}) + L_{\hat{g}}\hat{h}(\hat{x})\hat{u}_d(\hat{x}) + \alpha(\hat{h}(\hat{x}))}{L_{\hat{g}}\hat{h}(\hat{x})L_{\hat{g}}\hat{h}(\hat{x})^T + \gamma^{-1}\hat{h}(\hat{x})^2}, & \hat{x} \in \hat{\Omega}, \\ 0, & \hat{x} \notin \hat{\Omega}, \end{cases} \quad (54)$$

and

$$\hat{\Omega} = \{\hat{x} \in \mathbb{R}^n : L_{\hat{f}}\hat{h}(\hat{x}) + L_{\hat{g}}\hat{h}(\hat{x})\hat{u}_d(\hat{x}) + \alpha(\hat{h}(\hat{x})) < 0\}. \quad (55)$$

Figure 7 illustrates the architecture of the control (37), (38), (46)–(49), and (53)–(55). The following corollary is the main result on using this control for safety with input constraints. This corollary is obtained by applying Theorem 2 to the cascade (40)–(42).

Corollary 3. Consider (2), where (A1) is satisfied, and consider u given by (37), (38), (46)–(49), and (53)–(55), where (C1) and (C2) are satisfied. Assume that \hat{h}' is locally Lipschitz on $\hat{\mathcal{S}}$, and for all $\hat{x} \in \hat{\mathcal{B}}$, $L_{\hat{g}}\hat{h}(\hat{x}) \neq 0$. Let $\hat{x}_0 \in \hat{\mathcal{S}}$. Then, for all $t \in I(\hat{x}_0)$, $\hat{x}(t) \in \hat{\mathcal{S}}$, $x(t) \in \mathcal{S}_s$, and $u(t) \in \mathcal{U}$.

E. Ground Robot Example Revisited with Input Constraints

We present examples to demonstrate the control (37), (38), (46)–(49), and (53)–(55). The first example compares this control to an approach that uses multiple HOCBFs constraints in combination with input constraints.

Example 4. We consider the nonholonomic ground robot from Example 1, and the map shown in Figure 8, which has one obstacle. The area outside the obstacle is modeled by the zero-superlevel set of

$$h_1(x) = 1 - \|[q_x \quad q_y]^T\|_2/4.$$

The bounds on speed v are modeled as the the zero-superlevel sets of

$$h_2(x) = v + 0.5, \quad h_3(x) = v - 2.$$

We also consider input constraints. Specifically, the control must remain in the admissible set \mathcal{U} given by (32), where

$$\begin{aligned} \phi_1(u) &= 2 - u_1, & \phi_2(u) &= u_1 + 2, \\ \phi_3(u) &= 1 - u_2, & \phi_4(u) &= u_2 + 1, \end{aligned}$$

which implies $\mathcal{U} = \{u \in \mathbb{R}^2 : |u_1| \leq 2 \text{ and } |u_2| \leq 1\}$. The desired control u_d and cost (9) are the same as in Example 1. Thus, u_d is given by (28)–(31); and we consider the cost (9), where $Q(x) = I_2$ and $c(x) = -u_d(x)$, which is the minimum-intervention problem. We compare 2 control approaches.

The first approach is the soft-minimum R-CBF control (37), (38), (46)–(49), and (53)–(55). We use the control dynamics (37) and (38), where f_c , g_c , and h_c are given by Example 3 with $A_c = \begin{bmatrix} -1 & 0 \\ 0 & -0.6 \end{bmatrix}$, $B_c = -A_c$, and $C_c = I_2$. Thus, the control dynamics are LTI and low pass. Conditions (C1) and (C2) are satisfied with $d_c = 1$ and $\zeta = 1$, and (45) implies that $\hat{\ell} = 7$, $\hat{d}_1 = 3$, $\hat{d}_2 = \hat{d}_3 = 2$, $\hat{d}_4 = \hat{d}_5 = \hat{d}_6 = \hat{d}_7 = 1$. We implement the control (37), (38), (46)–(49), and (53)–(55) with $\gamma = 100$, $\hat{\alpha}_{1,0}(h) = 50h$, $\hat{\alpha}_{1,1}(h) = \hat{\alpha}_{2,0}(h) = \hat{\alpha}_{3,0}(h) = \alpha(h) = h$, and $x_{c0} = [0 \quad 0]^T$. All other parameters are the same as in Example 1.

The second approach generates the control from a quadratic program with multiple HOCBF constraints and explicit input constraints (e.g., see [49]). Specifically, the control u and

slack variables μ_1, μ_2, μ_3 are computed by minimizing the cost

$$J_{\text{HOCBF}}(u, \mu_1, \mu_2, \mu_3) = \|u - u_d(x)\|_2^2 + \frac{1}{2} \sum_{j=1}^3 \gamma_j \mu_j^2,$$

subject $u \in \mathcal{U}$ and

$$\begin{aligned} L_f b_{1,1}(x) + L_g b_{1,1}(x)u + \alpha_1(b_{1,1}(x)) + \mu_1 b_{1,1}(x) &\geq 0, \\ L_f h_2(x) + L_g h_2(x)u + \alpha_2(h_2(x)) + \mu_2 h_2(x) &\geq 0, \\ L_f h_3(x) + L_g h_3(x)u + \alpha_3(h_3(x)) + \mu_3 h_3(x) &\geq 0, \end{aligned}$$

where $b_{1,1}$ is given by (10) with $\alpha_{1,0}(h) = 50h$, $\gamma_1 = \gamma_2 = \gamma_3 = 100$, and $\alpha_1(h) = \alpha_2(h) = \alpha_3(h) = h$. Both methods are implemented at 50 Hz.

Figure 8 shows the closed-loop trajectories for both methods with $x_0 = [-3 \ -2 \ 1 \ \frac{\pi}{4}]^T$ and the goal location $q_d = [3 \ 3]^T$, and Figures 9 and 10 show the time histories of h_j and u . Figures 8 and 9 demonstrates that the multiple-HOCBF method does not satisfy safety; the robot collides with the obstacle at $t = 1.24$ s. This failure occurs because the state and input constraints in the multiple-HOCBF method are completely independent. Thus, the robot is able to enter a subset of the state space, where collision becomes unavoidable. As shown in Figure 10, the controls saturate prior to the collision but there is insufficient control authority to avoid collision. In contrast, the soft-minimum R-CBF method uses the control dynamics and soft-minimum R-CBF to integrate all constraints and guarantee safety. As shown in Figures 8–10, the trajectory with the soft-minimum R-CBF method satisfies the safety and input constraints, and the robot reaches its destination.

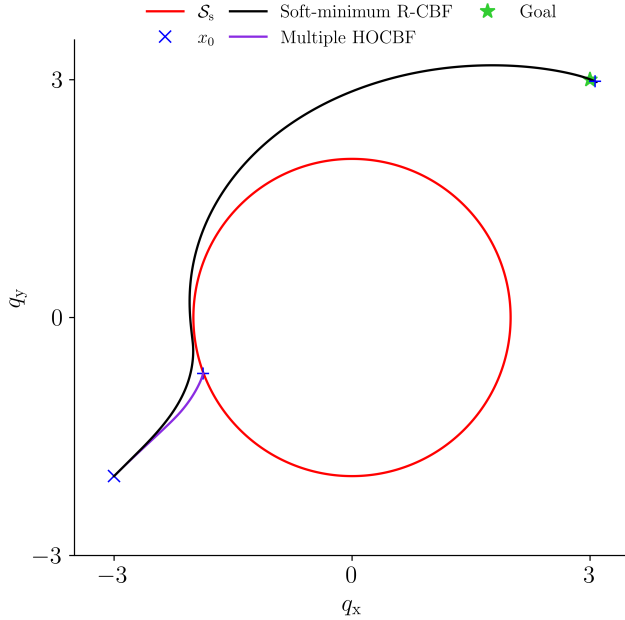


FIGURE 8. Closed-loop trajectories for soft-minimum R-CBF and multiple-HOCBF methods

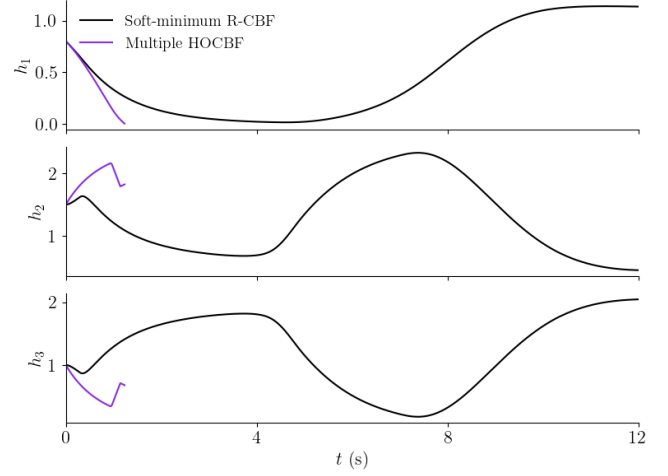


FIGURE 9. h_1, h_2 , and h_3 for soft-minimum R-CBF and multiple-HOCBF methods

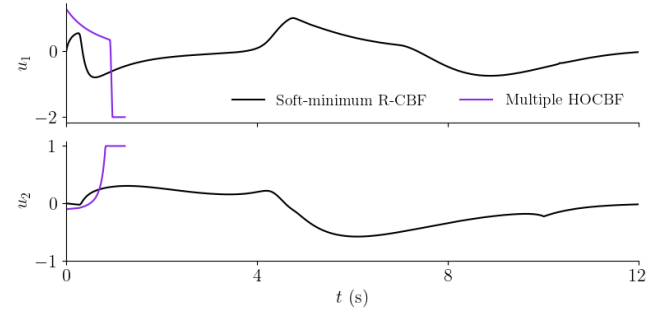


FIGURE 10. u for soft-minimum R-CBF and multiple-HOCBF methods

In this simple example, it is possible to prevent collision with the multiple-HOCBF method by selecting more conservative values for $\gamma_1, \gamma_2, \gamma_3, \alpha_1, \alpha_2$, and α_3 . However, this is problem specific, and it may not be possible to select conservative enough tuning in more complicated scenarios. Moreover, it is difficult to determine if a specific tuning is conservative enough to result in safe trajectories. In contrast, Corollary 3 shows that the soft-minimum R-CBF method is safe for any choice of parameters. \triangle

The next example revisits Example 1 but includes input constraints as well as safety constraints.

Example 5. We revisit the nonholonomic ground robot from Example 1 and include not only safety constraints but also input constraints. The safe set \mathcal{S}_s , desired control u_d , and cost (9) are the same as in Example 1. Thus, h_1, \dots, h_9 are given by (25)–(27); u_d is given by (28)–(31); and we consider the cost (9), where $Q(x) = I_2$ and $c(x) = -u_d(x)$, which is the minimum-intervention problem.

We also consider input constraints. Specifically, the control must remain in the admissible set \mathcal{U} is given by (32), where

$$\begin{aligned} \phi_1(u) &= 4 - u_1, & \phi_2(u) &= u_1 + 4, \\ \phi_3(u) &= 1 - u_2, & \phi_4(u) &= u_2 + 1, \end{aligned}$$

which implies $\mathcal{U} = \{u \in \mathbb{R}^2: |u_1| \leq 4 \text{ and } |u_2| \leq 1\}$ and $\hat{\ell} = 13$.

We use the low-pass LTI control dynamics from Example 4, and (45) implies that $\hat{d}_1 = \dots = \hat{d}_7 = 3$, $\hat{d}_8 = \hat{d}_9 = 2$, and $\hat{d}_{10} = \dots = \hat{d}_{13} = 1$. We implement the control (37), (38), (46)–(49), and (53)–(55) with $\rho = 10$, $\gamma = 200$, $\hat{\alpha}_{1,0}(h) = \dots = \hat{\alpha}_{7,0}(h) = h$, $\hat{\alpha}_{1,1}(h) = \dots = \hat{\alpha}_{6,1}(h) = 2.5h$, $\hat{\alpha}_{7,1}(h) = h$, $\hat{\alpha}_{8,0}(h) = \hat{\alpha}_{9,0}(h) = 10h$, $\alpha(h) = h$, and $\sigma_0 = 0.5$. For sample-data implementation, the control is updated at 50 Hz.

Figure 11 2,500 closed-loop trajectories for $x_0 = [-1 \ -8.5 \ 0 \ \frac{\pi}{2}]^T$, $x_{c0} = [0 \ 0]^T$, and randomly distributed goal locations. For each case, all safety and input constraints are satisfied along the closed-loop trajectory. As discussed in Example 1, increasing the gains k_1, k_2, k_3 in the desired control (28)–(31) tends to enlarge the set of reachable goal locations. Similar results where all state and input constraints are satisfied can be obtained with different choices of $\gamma > 0$, $\alpha_{j,1}, \dots, \alpha_{j,d_j-2}$, and α . These user-selected values impact the aggressiveness of the control.

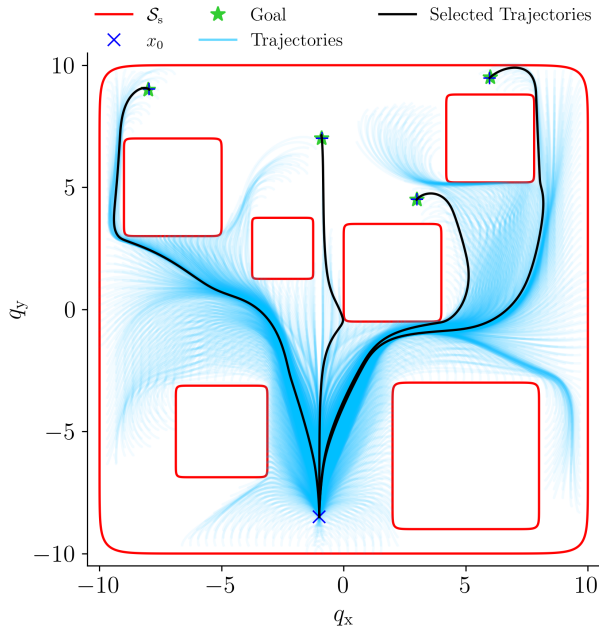


FIGURE 11. Safe set \mathcal{S}_s , and 2,500 closed-loop trajectories using the control (37), (38), (46)–(49), and (53)–(55).

Figure 11 also highlights the closed-loop trajectories for 4 selected goal locations: $q_d = [3 \ 4.5]^T$, $q_d = [-8 \ 9]^T$, $q_d = [6 \ 9.5]^T$, and $q_d = [-1 \ 7]^T$. Figures 12 and 13 show the trajectories of the relevant signals for the case where $q_d = [3 \ 4.5]^T$. Figure 13 shows that \hat{h} , $\min \hat{b}_{j,i}$, and $\min \hat{h}_j$ are positive for all time, which implies that x remains in \mathcal{S}_s and u remains in \mathcal{U} . \triangle

VII. Concluding Remarks

This article presents several contributions. Section IV presents and analyzes a method for constructing a composite

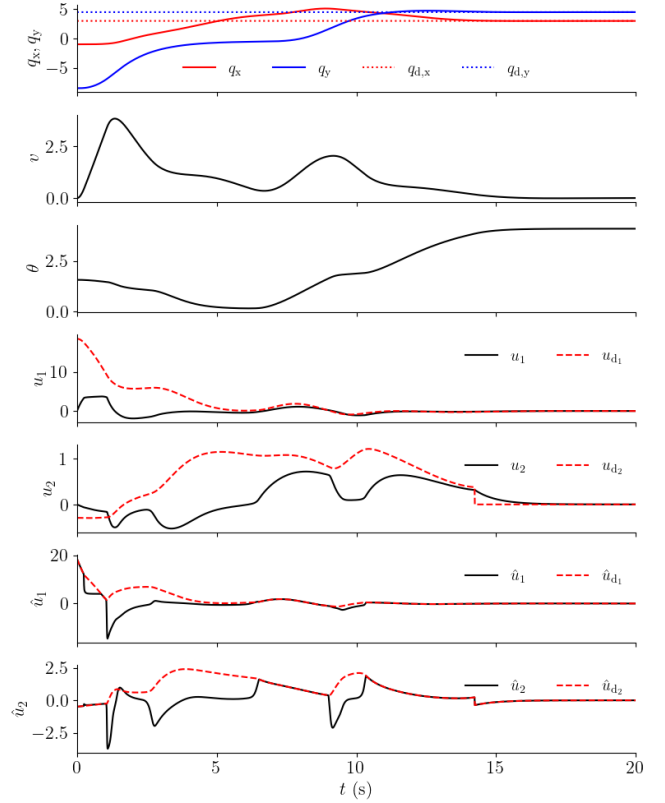


FIGURE 12. $q_x, q_y, v, \theta, u, u_d, \hat{u} = [\hat{u}_1 \ \hat{u}_2]^T$, and $\hat{u}_d = [\hat{u}_{d1} \ \hat{u}_{d2}]^T$ for $q_d = [3 \ 4.5]^T$.

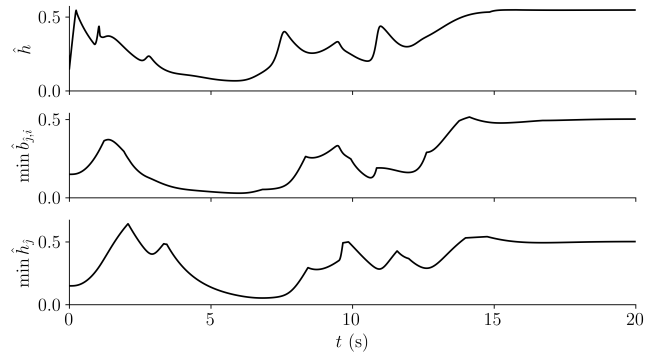


FIGURE 13. \hat{h} , $\min \hat{b}_{j,i}$, and $\min \hat{h}_j$ for $q_d = [3 \ 4.5]^T$.

soft-minimum R-CBF (14) from multiple CBFs, which can have different relative degrees. Proposition 3 is the main result of Section IV, and it shows that the soft-minimum R-CBF describes a control forward invariant set \mathcal{S} , which is a subset of the safe set \mathcal{S}_s . Next, Section V uses the composite soft-minimum R-CBF (14) in a constrained quadratic optimization to construct a closed-form optimal control that guarantees safety. Theorem 2 is the main result of Section V, and this theorem shows that the closed-form optimal control guarantees safety.

Section VI presents the main result of this article, which is a closed-form optimal control that not only guarantees

safety but also respects input constraints. The key elements in the development of this control include the introduction of the control dynamics (37) and (38) to transform the input constraint into state constraints; the use of the soft-minimum R-CBF to compose safety and input constraints, which have different relative degrees; and the introduction of a desired surrogate control (49) and associate surrogate cost (51). Corollary 3 is the main result, which shows that the closed-form optimal control (37), (38), (46)–(49), and (53)–(55) guarantees both safety- and input-constraint satisfaction.

One limitation of the method in this article is the assumption that $L_{\hat{g}}\hat{h}$ is nonzero on $\hat{\mathcal{B}}$, which is a subset of the boundary of the zero-superlevel set of the soft-minimum R-CBF \hat{h} . In many instances, this condition can be verified numerically. In addition, Proposition 5 provides a sufficient condition such that this assumption is satisfied. However, determining easy to verify necessary and sufficient conditions is open for future work. Moreover, an analysis of the restrictiveness of this assumption as compared to the typical CBF assumption (A1) is an open question.

The control for safety with input constraints depends on the choice of control dynamics (37) and (38). Safety is guaranteed for any control dynamics that satisfy (C1) and (C2); however, the specific choice can impact performance. The examples in this article demonstrate that low-pass LTI control dynamics can be effective. It is reasonable to design the control dynamics as LTI and low pass or band pass based on the specific control objective (i.e., u_d). However, other designs of the control dynamics (37) and (38) may yield superior performance with respect to the cost J . Analyzing the design of (37) and (38) based on the performance objective is an open question. Additionally, it may be possible to design (37) and (38) in order to positively impact satisfaction of the assumption that $L_{\hat{g}}\hat{h}$ is nonzero on $\hat{\mathcal{B}}$. This too is open for future work.

The approach to safety and input constraints can be directly extended to address input rate constraints (and constraints on higher-order time derivatives of the input). To accomplish this, the control dynamics (37) and (38) are designed such that its relative degree d_c is greater than the positive integer r , where $\frac{d^r}{dt^r}u$ is the highest-order time derivative of the control that has a constraint. In this case, constraints on $u, \frac{d}{dt}u, \dots, \frac{d^r}{dt^r}u$ are transformed into constraints on the controller state x_c using the approach in Section VI.

In this work, the soft minimum is used as a smooth approximation of the minimum. If $\rho > 0$ is small, then the soft minimum is a conservative approximation of the minimum. In this case, $\hat{\mathcal{H}}$ is a conservative approximation of $\bigcap_{j=1}^{\hat{\ell}} \hat{\mathcal{C}}_{j, \hat{d}_j-1}$. Thus, it is desirable to select $\rho > 0$ large. However, there are practical limits to the magnitude of ρ . If $\rho > 0$ is large, then $\|\hat{h}'(x)\|_2$ is large at points where the minimum function is not differentiable, which can result in the surrogate control \hat{u} having time derivatives with large magnitudes. Thus, selecting ρ is a trade-off between the conservativeness of \hat{h} and the size of $\|\hat{h}'(x)\|_2$.

In this work, the log-sum-exponential soft minimum (1) is used to compose multiple state constraints and multiple input constraints into a single constraint. In other words, the zero-superlevel set of the soft minimum (1) is an approximation (subset) of the intersection of the zero-superlevel sets of the arguments of the soft minimum. See Proposition 2. Thus, the log-sum-exponential soft minimum can be used to approximate the intersection of zero-superlevel sets. Similarly, the log-sum-exponential soft maximum can be used to approximate the union of zero-superlevel sets. See [30] for more details.

Appendix A Proof of Propositions 1 and 6–8

Proof of Proposition 1:

Define $z_{\min} \triangleq \min\{z_1, z_2, \dots, z_N\}$. Since the exponential is nonnegative and strictly increasing, it follows that

$$e^{-\rho z_{\min}} \leq \sum_{i=1}^N e^{-\rho z_i} \leq N e^{-\rho z_{\min}},$$

and taking the logarithm yields

$$-\rho z_{\min} \leq \log \sum_{i=1}^N e^{-\rho z_i} \leq \log N - \rho z_{\min}.$$

Then, dividing by $-\rho$ yields the result. ■

Proof of Proposition 6:

Let $t_1 \in I(\hat{x}_0)$. Since $\hat{x}(t_1) \in \hat{\mathcal{S}}_s$, it follows from (43) that $x(t_1) \in \mathcal{S}_s$ and $x_c(t_1) \in \mathcal{S}_c$. Since $x_c(t_1) \in \mathcal{S}_c$, it follows from (38) and (39) that $u(t_1) \in \mathcal{U}$. ■

Proof of Proposition 7:

Let $a \in \{1, 2, \dots, \ell\}$, and it follows from (A1) and (C1) that (A2) in Appendix B is satisfied for $x_1, x_2, f_1, g_1, f_2, g_2, \mathcal{X}_1, \mathcal{X}_2, \xi_1, \xi_2, r_1, r_2$ equal to $x, x_c, f, g, f_c, g_c, \mathbb{R}^n, \mathbb{R}^{n_c}, h_a, h_c, d_a, d_c$, respectively. Thus, it follows from Theorem 3 in Appendix B that $L_{\hat{g}}\hat{h}_a(\hat{x}) = \dots = L_{\hat{g}}L_{\hat{f}}^{d_a+d_c-2}\hat{h}_a(\hat{x}) = 0$ and $L_{\hat{g}}L_{\hat{f}}^{d_a+d_c-1}\hat{h}_a(\hat{x}) = [L_{\hat{g}}L_{\hat{f}}^{d_a-1}h_a(x)]L_{g_c}L_{f_c}^{d_c-1}h_c(x_c)$. Since, in addition, (A1) implies that for all $x \in \mathcal{S}_s$, $L_{\hat{g}}L_{\hat{f}}^{d_a-1}h_a(x) \neq 0$ and (C1) implies that for all $x \in \mathbb{R}^{n_c}$, $L_{g_c}L_{f_c}^{d_c-1}h_c(x_c)$ is nonsingular, it follows that for all $\hat{x} \in \hat{\mathcal{S}}_s$, $L_{\hat{g}}L_{\hat{f}}^{d_a+d_c-1}\hat{h}_a(\hat{x}) \neq 0$, which confirms the result for $\hat{j} \in \{1, 2, \dots, \ell\}$.

Let $b \in \{\ell + 1, \ell + 2, \dots, \hat{\ell}\}$ and let $i \in \{0, 1, \dots, \zeta - 1\}$. Next, it follows from (41) that $L_{\hat{f}}^i\hat{h}_b(\hat{x}) = L_{\hat{f}}^i\phi_{b-\ell}(h_c(x_c)) = L_{\hat{f}}^{i-1}L_{f_c}\phi_{b-\ell}(h_c(x_c)) = \dots = L_{f_c}^i\phi_{b-\ell}(h_c(x_c))$, which combined with (42) implies that

$$L_{\hat{g}}L_{\hat{f}}^i\hat{h}_b(\hat{x}) = L_{\hat{g}}L_{f_c}^i\phi_{b-\ell}(h_c(x_c)) = L_{g_c}L_{f_c}^i\phi_{b-\ell}(h_c(x_c)).$$

Thus, (C2) implies that for all $\hat{x} \in \mathbb{R}^{\hat{n}}$, $L_{\hat{g}}\hat{h}_b(\hat{x}) = \dots = L_{\hat{g}}L_{\hat{f}}^{\zeta-2}\hat{h}_b(\hat{x}) = 0$ and for all $\hat{x} \in \hat{\mathcal{S}}_s$, $L_{\hat{g}}L_{\hat{f}}^{\zeta-1}\hat{h}_b(\hat{x}) \neq 0$, which combined with (45) confirms the result for $\hat{j} \in \{\ell + 1, \ell + 2, \dots, \hat{\ell}\}$. ■

Proof of Proposition 8:

To prove (a), it follows from (C1) that the d_c th time derivative of u along (37) and (38) is $u^{(d_c)} = L_{f_c}^{d_c} h_c(x_c) + L_{g_c} L_{f_c}^{d_c-1} h_c(x_c) \hat{u}(\hat{x})$. Since, in addition, $\hat{u} = \hat{u}_d$ and $\sigma_{d_c} = 1$, substituting (49) yields

$$\frac{d^{d_c}}{dt^{d_c}} u = L_{\hat{f}}^{d_c} u_d(\hat{x}) + \sum_{i=0}^{d_c-1} \sigma_i \left(L_{\hat{f}}^i u_d(\hat{x}) - L_{f_c}^i h_c(x_c) \right). \quad (56)$$

Next, (A1) and (C1) imply that (A2) in Appendix B is satisfied for $x_1, x_2, f_1, g_1, f_2, g_2, \mathcal{X}_1, \mathcal{X}_2, \xi_1, \xi_2, r_1, r_2$ equal to $x, x_c, f, g, f_c, g_c, \mathbb{R}^n, \mathbb{R}^{n_c}, h_j, h_c, d_j, d_c$, respectively. Thus, it follows from Lemma 5 in Appendix B with $\hat{v} = u_d$ that $L_{\hat{g}} u_d(\hat{x}) = L_{\hat{g}} L_{\hat{f}} u_d(\hat{x}) = \dots = L_{\hat{g}} L_{\hat{f}}^{d_c-1} u_d(\hat{x}) = 0$. Thus, for $i \in \{0, 1, \dots, d_c\}$, the i th time derivative of (48) along (40)–(42) is

$$\frac{d^i}{dt^i} u_d(\hat{x}) = L_{\hat{f}}^i u_d(\hat{x}). \quad (57)$$

Similarly, for $i \in \{0, 1, \dots, d_c - 1\}$, it follows from (C1) that the i th time derivative of (38) along (37) is

$$\frac{d^i}{dt^i} u = L_{f_c}^i h_c(x_c). \quad (58)$$

Finally, substituting (57) and (58) into (56) yields (50), which confirms (a).

To prove (b), since all roots of σ are in the open left-hand complex plane, it follows from (50) that for all $\hat{x}_0 \in \mathbb{R}^{\hat{n}}$, $\lim_{t \rightarrow \infty} [u(t) - u_d(\hat{x}(t))] = 0$ exponentially, which confirms (b).

To prove (c), define $u_e \triangleq u - u_d(\hat{x})$. Thus, $u = u_e + u_d(\hat{x})$, and it follows from (9) and (48) that

$$\begin{aligned} J(x, u) &= \frac{1}{2} (u_e + u_d(\hat{x}))^T Q(x) (u_e + u_d(\hat{x})) \\ &\quad + c(x)^T (u_e + u_d(\hat{x})) \\ &= \frac{1}{2} u_e^T Q(x) u_e + u_d(\hat{x})^T Q(x) u_e + c(x)^T u_e \\ &\quad + \frac{1}{2} u_d(\hat{x})^T Q(x) u_d(\hat{x}) + c(x)^T u_d(\hat{x}) \\ &= \frac{1}{2} u_e^T Q(x) u_e + J(x, u_d(\hat{x})) \end{aligned}$$

which implies that $J(x, u) - J(x, u_d(\hat{x})) = \frac{1}{2} u_e^T Q(x) u_e$. Since, in addition, $\lim_{t \rightarrow \infty} u_e(t) = 0$ and Q is bounded, it follows that $\lim_{t \rightarrow \infty} [J(x(t), u(t)) - J(x(t), u_d(\hat{x}(t)))] = 0$, which confirms (c).

To prove (d), since for $i \in \{0, 1, \dots, d_c - 1\}$, $L_{f_c}^i h_c(x_{c0}) = L_{\hat{f}}^i u_d(\hat{x}_0)$, it follows from (57) and (58) that for $i \in \{0, 1, \dots, d_c - 1\}$, $\frac{d^i}{dt^i} u(t)|_{t=0} = \frac{d^i}{dt^i} u_d(\hat{x}(t))|_{t=0}$, which combined with (50), implies that $u(t) \equiv u_d(\hat{x}(t))$. ■

Appendix B Relative Degree of a Nonlinear Cascade

This appendix examines the relative degree of a cascade of nonlinear systems. The results in this appendix are needed for Proposition 7 and Proposition 8 in Section VI. Consider

$$\dot{x}_1(t) = f_1(x_1(t)) + g_1(x_1(t))u_1(t), \quad (59)$$

$$\dot{x}_2(t) = f_2(x_2(t)) + g_2(x_2(t))u_2(t), \quad (60)$$

where for $i \in \{1, 2\}$, $x_i(t) \in \mathbb{R}^{n_i}$ is the state, $x_i(0) = x_{i0} \in \mathbb{R}^{n_i}$ is the initial condition, and $u_i(t) \in \mathbb{R}^{m_i}$ is the input.

Let $\xi_1 : \mathbb{R}^{n_1} \rightarrow \mathbb{R}^{\ell_1}$ and $\xi_2 : \mathbb{R}^{n_2} \rightarrow \mathbb{R}^{m_1}$. We make the following assumption:

(A2) For $i \in \{1, 2\}$, there exists $\mathcal{X}_i \subseteq \mathbb{R}^{n_i}$ and a positive integer r_i such that for all $x_i \in \mathcal{X}_i$, $L_{g_i} \xi_i(x_i) = L_{g_i} L_{f_i} \xi_i(x_i) = \dots = L_{g_i} L_{f_i}^{r_i-2} \xi_i(x_i) = 0$.

Assumption (A2) implies that if $a_i \in \mathcal{X}_i$ and $L_{g_i} L_{f_i}^{r_i-1} \xi_i(a_i) \neq 0$, then ξ_i has relative degree r_i with respect to $\dot{x}_i = f_i(x_i) + g_i(x_i)u_i$ at a_i .

Next, we consider the cascade of (59) and (60), where $u_1 = \xi_2(x_2)$, which is given by

$$\dot{\hat{x}} = \hat{f}(\hat{x}) + \hat{g}(\hat{x})u_2, \quad (61)$$

$$y = \hat{h}(\hat{x}), \quad (62)$$

where

$$\hat{x} \triangleq \begin{bmatrix} x_1 \\ x_2 \end{bmatrix}, \quad \hat{f}(\hat{x}) \triangleq \begin{bmatrix} f_1(x_1) + g_1(x_1)\xi_2(x_2) \\ f_2(x_2) \end{bmatrix}, \quad (63)$$

$$\hat{g}(\hat{x}) \triangleq \begin{bmatrix} 0 \\ g_2(x_2) \end{bmatrix}, \quad \hat{h}(\hat{x}) \triangleq \xi_1(x_1). \quad (64)$$

The following preliminary results are needed.

Lemma 3. Consider (59)–(64), where (A2) is satisfied. For all $\hat{x} \in \mathcal{X}_1 \times \mathcal{X}_2$, the following statements hold:

- (a) Let $j \in \{0, 1, \dots, r_1 - 1\}$. Then, $L_{\hat{f}}^j \hat{h}(\hat{x}) = L_{f_1}^j \xi_1(x_1)$.
- (b) Let $j \in \{0, 1, \dots, r_1 - 2\}$. Then, $L_{\hat{g}} L_{\hat{f}}^j \hat{h}(\hat{x}) = 0$.

Proof:

To prove (a), we use induction on j . First, note that $L_{\hat{f}}^0 \hat{h}(\hat{x}) = \hat{h}(\hat{x}) = \xi_1(x_1) = L_{f_1}^0 \xi_1(x_1)$, which implies that (a) holds for $j = 0$. Next, assume that (a) holds for $j = a \in \{0, 1, \dots, r_1 - 2\}$. Thus,

$$L_{\hat{f}}^{a+1} \hat{h}(\hat{x}) = L_{\hat{f}} L_{\hat{f}}^a \hat{h}(\hat{x}) = L_{\hat{f}} L_{f_1}^a \xi_1(x_1),$$

which combined with (63) and (A2) yields

$$\begin{aligned} L_{\hat{f}}^{a+1} \hat{h}(\hat{x}) &= L_{f_1}^{a+1} \xi_1(x_1) + [L_{g_1} L_{f_1}^a \xi_1(x_1)] \xi_2(x_2) \\ &= L_{f_1}^{a+1} \xi_1(x_1), \end{aligned}$$

which confirms (a).

To prove (b), let $b \in \{0, 1, \dots, r_1 - 2\}$, and it follows from (a) that $L_{\hat{g}} L_{\hat{f}}^b \hat{h}(\hat{x}) = L_{\hat{g}} L_{f_1}^b \xi_1(x_1) = 0$. ■

Let $\nu : \mathbb{R}^{n_1} \rightarrow \mathbb{R}^{\ell_1}$ be continuously differentiable, and let $\hat{\nu} : \mathbb{R}^{n_1+n_2} \rightarrow \mathbb{R}^{\ell_1}$ be defined by $\hat{\nu}(\hat{x}) \triangleq \nu(x_1)$.

Lemma 4. Let j be a positive integer. Then, there exists $F_j : \mathbb{R}^{n_1 \times m_1^{j-1}} \rightarrow \mathbb{R}^{\ell_1}$ such that for all $\hat{x} \in \mathcal{X}_1 \times \mathcal{X}_2$,

$$\begin{aligned} L_{\hat{f}}^j \hat{\nu}(\hat{x}) &= F_j \left(x_1, \xi_2(x_2), L_{f_2} \xi_2(x_2), \dots, L_{f_2}^{j-2} \xi_2(x_2) \right) \\ &\quad + [L_{g_1} \nu(x_1)] L_{f_2}^{j-1} \xi_2(x_2). \end{aligned} \quad (65)$$

Proof:

We use induction on j . First, (63) implies that $L_{\hat{f}} \hat{\nu}(\hat{x}) = L_{\hat{f}} \nu(x_1) = L_{f_1} \nu(x_1) + [L_{g_1} \nu(x_1)] \xi_2(x_2) = F_1(x_1) +$

$[L_{g_1}\nu(x_1)]\xi_2(x_2)$, where $F_1(x_1) = L_{f_1}\nu(x_1)$, which confirms (65) for $j = 1$.

Next, assume that (65) holds for $j = a \in \{1, 2, \dots\}$. Thus,

$$\begin{aligned} L_{\hat{f}}^{a+1}\hat{\nu}(\hat{x}) &= L_{\hat{f}}L_{\hat{f}}^a\hat{\nu}(\hat{x}) \\ &= L_{\hat{f}}F_a + L_{\hat{f}}\left[L_{g_1}\nu(x_1)L_{f_2}^{a-1}\xi_2(x_2)\right], \end{aligned} \quad (66)$$

where the arguments of F_a are omitted. Next, note that it follows from (63) that

$$\begin{aligned} L_{\hat{f}}F_a &= \frac{\partial F_a}{\partial x_1}[f_1(x_1) + g_1(x_1)\xi_2(x_2)] \\ &\quad + \sum_{k=0}^{a-2} \frac{\partial F_a}{\partial L_{f_2}^k \xi_2} \frac{\partial L_{f_2}^k \xi_2(x_2)}{\partial x_2} f_2(x_2) \\ &= L_{f_1}F_a + [L_{g_1}F_a]\xi_2(x_2) + \sum_{k=0}^{a-2} \frac{\partial F_j}{\partial L_{f_2}^k \xi_2} L_{f_2}^{k+1}\xi(x_2). \end{aligned} \quad (67)$$

and

$$\begin{aligned} L_{\hat{f}}\left[L_{g_1}\nu(x_1)L_{f_2}^{a-1}\xi_2(x_2)\right] &= \left(I_{\ell_1} \otimes L_{f_2}^{a-1}\xi_2(x_2)\right)^T G(x_1) \\ &\quad \times (f_1(x_1) + g_1(x_1)\xi_2(x_2)) \\ &\quad + L_{g_1}\nu(x_1)L_{f_2}^a\xi_2(x_2), \end{aligned} \quad (68)$$

where \otimes is the Kronecker product,

$$G(x_1) \triangleq \begin{bmatrix} \frac{\partial}{\partial x_1}[L_{g_1}\nu(x_1)]_{(1)}^T \\ \vdots \\ \frac{\partial}{\partial x_1}[L_{g_1}\nu(x_1)]_{(\ell_1)}^T \end{bmatrix},$$

and $[L_{g_1}\nu(x_1)]_{(i)}$ is the i th row of $L_{g_1}\nu(x_1)$. Thus, substituting (67) and (68) into (66) yields

$$L_{\hat{f}}^{a+1}\hat{\nu}(\hat{x}) = F_{a+1} + L_{g_1}\nu(x_1)L_{f_2}^a\xi_2(x_2),$$

where

$$\begin{aligned} F_{a+1} &= L_{f_1}F_a + [L_{g_1}F_a]\xi_2(x_2) + \sum_{k=0}^{a-2} \frac{\partial F_j}{\partial L_{f_2}^k \xi_2} L_{f_2}^{k+1}\xi(x_2) \\ &\quad + \left(I_{\ell_1} \otimes L_{f_2}^{a-1}\xi_2(x_2)\right)^T G(x_1) \\ &\quad \times (f_1(x_1) + g_1(x_1)\xi_2(x_2)), \end{aligned}$$

which confirms (65) for $j = a + 1$. \blacksquare

Lemma 5. Consider (59)–(64), where (A2) is satisfied. For all $\hat{x} \in \mathcal{X}_1 \times \mathcal{X}_2$, the following statements hold:

- (a) For $j \in \{0, 1, \dots, r_2 - 1\}$, $L_{\hat{g}}L_{\hat{f}}^j\hat{\nu}(\hat{x}) = 0$.
- (b) $L_{\hat{g}}L_{\hat{f}}^{r_2}\hat{\nu}(\hat{x}) = [L_{g_1}\nu(x_1)]L_{g_2}L_{f_2}^{r_2-1}\xi_2(x_2)$.

Proof:

It follows from Lemma 4 that for all positive integers a ,

$$\begin{aligned} L_{\hat{g}}L_{\hat{f}}^a\hat{\nu}(\hat{x}) &= L_{\hat{g}}F_a(x_1, L_{f_2}^0\xi_2(x_2), \dots, L_{f_2}^{a-2}\xi_2(x_2)) \\ &\quad + L_{\hat{g}}\left([L_{g_1}\nu(x_1)]L_{f_2}^{a-1}\xi_2(x_2)\right). \end{aligned} \quad (69)$$

To prove (a), let $j \in \{0, 1, \dots, r_2 - 1\}$. Note that (64) and (A2) imply that $L_{\hat{g}}F_j(x_1, \xi_2(x_2), \dots, L_{f_2}^{j-2}\xi_2(x_2)) = 0$ and $L_{\hat{g}}([L_{g_1}\nu(x_1)]L_{f_2}^{j-1}\xi_2(x_2)) = 0$, which together with (69) confirms (a).

To prove (b), it follows from (64) and (A2) that $L_{\hat{g}}F_{r_2}(x_1, \xi_2(x_2), \dots, L_{f_2}^{r_2-2}\xi_2(x_2)) = 0$ and $L_{\hat{g}}([L_{g_1}\nu(x_1)]L_{f_2}^{r_2-1}\xi_2(x_2)) = [L_{g_1}\nu(x_1)]L_{g_2}L_{f_2}^{r_2-1}\xi_2(x_2)$, which together with (69) confirms (a). \blacksquare

The next theorem is the main result on the relative degree of a cascade of nonlinear systems. The result shows that if ξ_i has relative degree r_i with respect to $\dot{x}_i = f_i(x_i) + g_i(x_i)u_i$ at $a_i \in \mathcal{X}_i$, then the relative degree of the cascade (61)–(64) is greater than or equal to $r_1 + r_2$. Furthermore, the relative degree of the cascade (61)–(64) is $r_1 + r_2$ if and only if $[L_{g_1}L_{f_1}^{r_1-1}h_1(a_1)]L_{g_2}L_{f_2}^{r_2-1}h_2(a_2)$ is nonzero.

Theorem 3. Consider (59)–(64), where (A2) is satisfied. Then, for all $\hat{x} \in \mathcal{X}_1 \times \mathcal{X}_2$, the following statements hold:

- (a) For all $j \in \{0, 1, \dots, r_1 + r_2 - 2\}$, $L_{\hat{g}}L_{\hat{f}}^j\hat{h}(\hat{x}) = 0$.
- (b) $L_{\hat{g}}L_{\hat{f}}^{r_1+r_2-1}\hat{h}(\hat{x}) = [L_{g_1}L_{f_1}^{r_1-1}\xi_1(x_1)]L_{g_2}L_{f_2}^{r_2-1}\xi_2(x_2)$.

Proof:

Define $\nu(x_1) \triangleq L_{f_1}^{r_1-1}\xi_1(x_1)$ and $\hat{\nu}(\hat{x}) \triangleq \nu(x_1)$.

To prove (a), it follows from Lemma 3 that for all $j \in \{0, \dots, r_1 - 2\}$, $L_{\hat{g}}L_{\hat{f}}^j\hat{h}(\hat{x}) = 0$.

Next, let $a \in \{r_1 - 1, r_1, \dots, r_1 + r_2 - 2\}$ and define $b \triangleq a - r_1 + 1$. Thus, $L_{\hat{g}}L_{\hat{f}}^a\hat{h}(\hat{x}) = L_{\hat{g}}L_{\hat{f}}^bL_{\hat{f}}^{r_1-1}\hat{h}(\hat{x}) = L_{\hat{g}}L_{\hat{f}}^b\hat{\nu}(\hat{x})$. Since, in addition, $b \in \{0, \dots, r_2 - 1\}$, it follows from Lemma 5 that $L_{\hat{g}}L_{\hat{f}}^b\hat{\nu}(\hat{x}) = 0$, which implies that for all $j \in \{r_1 - 1, r_1, \dots, r_1 + r_2 - 2\}$, $L_{\hat{g}}L_{\hat{f}}^j\hat{h}(\hat{x}) = 0$.

To prove (b), note that $L_{\hat{g}}L_{\hat{f}}^{r_1+r_2-1}\hat{h}(\hat{x}) = L_{\hat{g}}L_{\hat{f}}^{r_2}L_{\hat{f}}^{r_1-1}\hat{h}(\hat{x}) = L_{\hat{g}}L_{\hat{f}}^{r_2}\hat{\nu}(\hat{x})$. Thus, Lemma 5 implies that $L_{\hat{g}}L_{\hat{f}}^{r_1+r_2-1}\hat{h}(\hat{x}) = [L_{g_1}\nu(x_1)]L_{g_2}L_{f_2}^{r_2-1}\xi_2(x_2) = [L_{g_1}L_{f_1}^{r_1-1}\xi_1(x_1)]L_{g_2}L_{f_2}^{r_2-1}\xi_2(x_2)$. \blacksquare

REFERENCES

- [1] A. D. Ames, X. Xu, J. W. Grizzle, and P. Tabuada, "Control barrier function based quadratic programs for safety critical systems," *IEEE Trans. Autom. Contr.*, pp. 3861–3876, 2016.
- [2] X. Xu, P. Tabuada, J. W. Grizzle, and A. D. Ames, "Robustness of control barrier functions for safety critical control," *IFAC-PapersOnLine*, vol. 48, no. 27, pp. 54–61, 2015.
- [3] K. P. Wabersich and M. N. Zeilinger, "Predictive control barrier functions: Enhanced safety mechanisms for learning-based control," *IEEE Trans. Autom. Contr.*, 2022.
- [4] X. Xu, J. W. Grizzle, P. Tabuada, and A. D. Ames, "Correctness guarantees for the composition of lane keeping and adaptive cruise control," *IEEE Trans. Auto. Sci. and Eng.*, pp. 1216–1229, 2017.
- [5] P. Seiler, M. Jankovic, and E. Hellstrom, "Control barrier functions with unmodeled input dynamics using integral quadratic constraints," *IEEE Contr. Sys. Let.*, vol. 6, pp. 1664–1669, 2021.
- [6] J. Breeden and D. Panagou, "Robust control barrier functions under high relative degree and input constraints for satellite trajectories," *Automatica*, vol. 155, p. 111109, 2023.
- [7] Q. Nguyen and K. Sreenath, "Exponential control barrier functions for enforcing high relative-degree safety-critical constraints," in *Proc. Amer. Contr. Conf. (ACC)*. IEEE, 2016, pp. 322–328.

- [8] M. Z. Romdlony and B. Jayawardhana, “Stabilization with guaranteed safety using control Lyapunov–barrier function,” *Automatica*, vol. 66, pp. 39–47, 2016.
- [9] S. Prajna, A. Jadbabaie, and G. J. Pappas, “A framework for worst-case and stochastic safety verification using barrier certificates,” *IEEE Trans. Autom. Contr.*, pp. 1415–1428, 2007.
- [10] D. Panagou, D. M. Stipanović, and P. G. Voulgaris, “Distributed coordination control for multi-robot networks using Lyapunov-like barrier functions,” *IEEE Trans. Autom. Contr.*, pp. 617–632, 2015.
- [11] K. P. Tee, S. S. Ge, and E. H. Tay, “Barrier Lyapunov functions for the control of output-constrained nonlinear systems,” *Automatica*, pp. 918–927, 2009.
- [12] X. Jin, “Adaptive fixed-time control for MIMO nonlinear systems with asymmetric output constraints using universal barrier functions,” *IEEE Trans. Autom. Contr.*, pp. 3046–3053, 2018.
- [13] Q. Nguyen and K. Sreenath, “Safety-critical control for dynamical bipedal walking with precise footstep placement,” *IFAC-PapersOnLine*, pp. 147–154, 2015.
- [14] M. Srinivasan and S. Coogan, “Control of mobile robots using barrier functions under temporal logic specifications,” *IEEE Trans. on Rob.*, vol. 37, no. 2, pp. 363–374, 2020.
- [15] Z. Jian, Z. Yan, X. Lei, Z. Lu, B. Lan, X. Wang, and B. Liang, “Dynamic control barrier function-based model predictive control to safety-critical obstacle-avoidance of mobile robot,” in *Proc. Int. Rob. Autom. (ICRA)*. IEEE, 2023, pp. 3679–3685.
- [16] A. Safari and J. B. Hoagg, “Time-varying soft-maximum control barrier functions for safety in an a priori unknown environment,” *arXiv preprint arXiv:2310.05261*, 2023.
- [17] U. Borrmann, L. Wang, A. D. Ames, and M. Egerstedt, “Control barrier certificates for safe swarm behavior,” *IFAC-PapersOnLine*, pp. 68–73, 2015.
- [18] A. Singletary, A. Swann, Y. Chen, and A. D. Ames, “Onboard safety guarantees for racing drones: High-speed geofencing with control barrier functions,” *IEEE Rob. and Autom. Let.*, vol. 7, no. 2, pp. 2897–2904, 2022.
- [19] J. Seo, J. Lee, E. Baek, R. Horowitz, and J. Choi, “Safety-critical control with nonaffine control inputs via a relaxed control barrier function for an autonomous vehicle,” *IEEE Rob. and Auto. Let.*, vol. 7, no. 2, pp. 1944–1951, 2022.
- [20] A. Alan, A. J. Taylor, C. R. He, A. D. Ames, and G. Orosz, “Control barrier functions and input-to-state safety with application to automated vehicles,” *IEEE Trans. on Contr. Sys. Tech.*, 2023.
- [21] R. Wisniewski and C. Sloth, “Converse barrier certificate theorems,” *IEEE Trans. Autom. Contr.*, pp. 1356–1361, 2015.
- [22] L. Wang, D. Han, and M. Egerstedt, “Permissive barrier certificates for safe stabilization using sum-of-squares,” in *2018 Amer. Contr. Conf. (ACC)*, 2018, pp. 585–590.
- [23] A. Clark, “Verification and synthesis of control barrier functions,” in *Proc. Conf. Dec. Contr. (CDC)*, 2021, pp. 6105–6112.
- [24] A. Isaly, M. Ghanbarpour, R. G. Sanfelice, and W. E. Dixon, “On the feasibility and continuity of feedback controllers defined by multiple control barrier functions for constrained differential inclusions,” in *2022 Amer. Contr. Conf. (ACC)*. IEEE, 2022, pp. 5160–5165.
- [25] E. Pond and M. Hale, “Fast verification of control barrier functions via linear programming,” *arXiv preprint arXiv:2212.00598*, 2022.
- [26] X. Tan and D. V. Dimarogonas, “Compatibility checking of multiple control barrier functions for input constrained systems,” in *Proc. Conf. Dec. Contr. (CDC)*. IEEE, 2022, pp. 939–944.
- [27] T. Gurriet, M. Mote, A. Singletary, P. Nilsson, E. Feron, and A. D. Ames, “A scalable safety critical control framework for nonlinear systems,” *IEEE Access*, pp. 187 249–187 275, 2020.
- [28] Y. Chen, A. Singletary, and A. D. Ames, “Guaranteed obstacle avoidance for multi-robot operations with limited actuation: A control barrier function approach,” *IEEE Contr. Sys. Let.*, pp. 127–132, 2020.
- [29] P. Rabiee and J. B. Hoagg, “Soft-minimum barrier functions for safety-critical control subject to actuation constraints,” in *Proc. Amer. Contr. Conf. (ACC)*, 2023, pp. 2646–2651.
- [30] —, “Soft-minimum and soft-maximum barrier functions for safety with actuation constraints,” *arXiv preprint arXiv:2305.10620*, 2023.
- [31] M. Black and D. Panagou, “Consolidated control barrier functions: Synthesis and online verification via adaptation under input constraints,” *arXiv preprint arXiv:2304.01815*, 2023.
- [32] L. Lindemann and D. V. Dimarogonas, “Control barrier functions for signal temporal logic tasks,” *IEEE control systems letters*, vol. 3, no. 1, pp. 96–101, 2018.
- [33] P. Glotfelter, J. Cortés, and M. Egerstedt, “Nonsmooth barrier functions with applications to multi-robot systems,” *IEEE Contr. Sys. Let.*, vol. 1, no. 2, pp. 310–315, 2017.
- [34] P. Glotfelter, I. Buckley, and M. Egerstedt, “Hybrid nonsmooth barrier functions with applications to provably safe and composable collision avoidance for robotic systems,” *IEEE Robotics and Automation Letters*, vol. 4, no. 2, pp. 1303–1310, 2019.
- [35] P. Wieland and F. Allgöwer, “Constructive safety using control barrier functions,” *IFAC Proceedings Volumes*, vol. 40, no. 12, pp. 462–467, 2007.
- [36] W. S. Cortez and D. V. Dimarogonas, “On compatibility and region of attraction for safe, stabilizing control laws,” *IEEE Transactions on Automatic Control*, vol. 67, no. 9, pp. 4924–4931, 2022.
- [37] F. Borrelli, A. Bemporad, and M. Morari, *Predictive control for linear and hybrid systems*. Cambridge University Press, 2017.
- [38] A. Bemporad, F. Borrelli, M. Morari *et al.*, “Model predictive control based on linear programming—the explicit solution,” *IEEE transactions on automatic control*, vol. 47, no. 12, pp. 1974–1985, 2002.
- [39] P. Tøndel, T. A. Johansen, and A. Bemporad, “An algorithm for multi-parametric quadratic programming and explicit mpc solutions,” *Automatica*, vol. 39, no. 3, pp. 489–497, 2003.
- [40] W. Xiao, C. G. Cassandras, C. A. Belta, and D. Rus, “Control barrier functions for systems with multiple control inputs,” in *2022 Amer. Contr. Conf. (ACC)*. IEEE, 2022, pp. 2221–2226.
- [41] A. D. Ames, G. Notomista, Y. Wardi, and M. Egerstedt, “Integral control barrier functions for dynamically defined control laws,” *IEEE Contr. Sys. Let.*, vol. 5, no. 3, pp. 887–892, 2020.
- [42] P. Rabiee and J. B. Hoagg, “Composition of control barrier functions with differing relative degrees for safety under input constraints,” *arXiv preprint arXiv:2310.00363*, 2023.
- [43] F. Blanchini, S. Miani *et al.*, *Set-theoretic methods in control*. Springer, 2008, vol. 78.
- [44] Y. Tassa, N. Mansard, and E. Todorov, “Control-limited differential dynamic programming,” in *2014 IEEE International Conference on Robotics and Automation (ICRA)*. IEEE, 2014, pp. 1168–1175.
- [45] X. Tan, W. S. Cortez, and D. V. Dimarogonas, “High-order barrier functions: Robustness, safety, and performance-critical control,” *IEEE Trans. Autom. Contr.*, vol. 67, no. 6, pp. 3021–3028, 2021.
- [46] S. J. Wright, *Primal-dual interior-point methods*. SIAM, 1997.
- [47] A. Ben-Tal and A. Nemirovski, *Lectures on modern convex optimization: analysis, algorithms, and engineering applications*. SIAM, 2001.
- [48] A. De Luca, G. Oriolo, and M. Vendittelli, “Control of wheeled mobile robots: An experimental overview,” *RAMSETE*, pp. 181–226, 2002.
- [49] W. Xiao and C. Belta, “High-order control barrier functions,” *IEEE Trans. Autom. Contr.*, vol. 67, no. 7, pp. 3655–3662, 2021.
- [50] B. Amos and J. Z. Kolter, “Optnet: Differentiable optimization as a layer in neural networks,” in *International Conference on Machine Learning*. PMLR, 2017, pp. 136–145.